

mesenchymal types of cells, only BM-MSCs have been clinically utilized, having shown safety and modest efficacy; the efficacy was believed to be due to the paracrine effect of engrafted BM-MSCs on residual host cardiomyocytes [12] or neovascularization [13, 14]. However, if we were to find the method to increase the CTE of BM-MSCs and/or increase the paracrine effect of BM-MSCs, the efficacy of ongoing clinical BM-MSC-based therapy may be significantly advanced. As preferred culture methods to elicit the maximal response of the paracrine effect of human BM-MSCs were still undetermined, clinical studies might do not yet show a substantial paracrine effect of BM-MSCs.

In our previous data [15], we found that the CTE of MMCs had been increased dramatically by use of L-carnitine-containing medium, which is essential for mitochondrial free fatty acid metabolism. Cardiomyocytes require free fatty acid as a major energy source. Therefore, mitochondrial function may play an important role in expressing cardiomyocyte phenotype. In fact, the mitochondrial morphology of cardiomyocytes is quite different from its morphology in other organs [16]. The mitochondrial proteins are synthesized not only by its own DNA but also by the DNA of the host nucleus, that is, peroxisome proliferators-activated receptor- γ (PPAR- γ) and PPAR- γ coactivator-1 α are known to activate mitochondrial gene transcription [17]. From another point of view, we speculated that environmental stimulation may cause change in mitochondrial function that might affect the gene expression of the host nucleus DNA, which may also play a role in the CTE of MSCs.

In this study, we hypothesized that stimulation of PPAR- γ by pioglitazone may increase the CTE of human MSCs. We examined the effect of pioglitazone, as a PPAR- γ activator, on efficiency of cardiomyogenic transdifferentiation of human BM-MSCs, *in vitro* and *in vivo*.

MATERIALS AND METHODS

Isolation of Human Mesenchymal Cells

After informed consent was obtained, 15 ml of bone marrow aspirate was obtained from the iliac bone of a 41-year-old male as described previously [5]. The collected sample was cultured in Dulbecco's modified Eagle's medium high-glucose supplemented with 10% human serum and established MSCs (BM-MSCs). BM-MSCs of 10–20 population doublings were used in the present study. We performed bone marrow aspiration procedure for six times and there was no difference among the BM-MSCs obtained from each procedure.

Cardiomyogenic Induction and Chemical Agents

The method of cardiomyogenic induction *in vitro* was described previously [5, 8–10]. In short, enhanced green fluorescent protein (EGFP)-labeled BM-MSCs were cocultured with murine cardiomyocytes (see detail in supporting information Material and Methods). In this system, the incidence of cell fusion was around 0.3% [8, 9, 18] and the evidence of cell fusion-independent cardiomyogenesis was extensively shown in the previous study [5, 8, 9, 11]. In our pilot study, we have confirmed that the incidence of cell fusion was not affected by pioglitazone (0.2%). Human cells were preincubated with medium containing 3 μ M of pioglitazone for 2 weeks before coculture and/or culture with the pioglitazone-containing medium after coculture. In another experiment, we administrated 1 μ M of GW9662, a specific PPAR- γ blocker. Pioglitazone (10 mM) and GW9662 (1 mM) stock solutions were freshly prepared with dimethyl sulfoxide (DMSO) (Sigma) solution and added to the culture media to give a final concentration. Evaluation of efficiency of cardiomyogenic

transdifferentiation was described previously [8, 9, 11, 15]. In short, cocultivated BM-MSCs were enzymatically isolated, a smear sample was made, and then immunocytochemistry using mouse monoclonal antibody against anti-cardiac troponin-I (Trop-I, #4T21 Hytest, Euro, Finland, <http://www.hytest.fi/>) antibody was performed (described later). Isolated cells (spherical shape), in which Trop-I localized at the cytoplasm were considered as Trop-I-positive cells. The CTE was defined as the incidence of Trop-I/EGFP double-positive cells in EGFP-positive BM-MSCs.

Immunocytochemistry and Immunohistochemistry

A laser confocal microscope (FV1000, Olympus, Tokyo, Japan, <http://www.olympus.co.jp/>) was used. As described previously, samples were stained with Trop-I, with mouse monoclonal anti-human atrial natriuretic peptide (hANP) antibody (YLEM, MCV928), or with mouse monoclonal anti-sarcomeric α -actinin antibody (Sigma-Aldrich, St. Louis, MO, <http://www.sigmaaldrich.com/>) and rabbit polyclonal anti-connexin 43 (Cx43) antibody (Sigma) diluted 1:300 overnight at 4°C, then stained with tetramethylrhodamine isothiocyanate-conjugated anti-mouse IgG antibody (Sigma) and Cy5-conjugated anti-rabbit IgG antibody (Chemicon, Billerica, MA, <http://www.millipore.com/>) diluted 1:100, containing 4'-6-diamidino-2-phenylindole (Wako, Tokyo, Japan, <http://www.wako-chem.co.jp/>) at 1:300 for 30 minutes at 25°C–28°C.

Enzyme-Linked Immunosorbent Assay

Angiogenic humoral factors (angiogenin, angiotensin-2, epidermal growth factor [EGF], basic fibroblast growth factor [bFGF], heparin-binding EGF-like growth factor [HB-EGF], hepatocyte growth factor [HGF], leptin, platelet-derived growth factor-BB [PDGF-BB], phosphatidylinositol-glycan biosynthesis class F protein [PIGF], vascular endothelial growth factor [VEGF]) in culture medium supernatant (cultured with 10% serum containing medium for 7 days) were measured by enzyme-linked immunosorbent assay (ELISA). The assay was performed with Quantibody Human Angiogenesis Array I kit (RayBiotech, Inc., Norcross, GA, <http://www.raybiotech.com/>) and was conducted according to manufacturer recommended protocol.

Transplantation of Pioglitazone-Pretreated Marrow-Derived MSCs in Myocardial Infarction Model *In Vivo*

Myocardial infarction (MI) was induced in the open chests of anesthetized female F344 nude rats (Clea Japan, Inc.; 6 weeks of age) as described previously [9]. Two weeks after MI, 1–2 $\times 10^6$ of EGFP-labeled BM-MSCs were injected into the myocardium at the border zone of the MI. Two weeks after the first operation, rats with MI were randomized in a blind study of the following groups: the sham-operated group (sham), the control MI group (MI), the MI+plain BM-MSCs-transplanted group (BM), and the MI+pioglitazone-pretreated MSCs-transplanted group (p-BM). After cellular transplantation, pioglitazone (2.5 mg/kg/day) was orally administered in some of the experiments (po). Randomization occurred immediately before echocardiogram. Immediately before cell transplantation, two-dimensional and M-mode echocardiographic (8.5 MHz linear transducer; EnVisor C, Philips Medical Systems, Andover, MA, <http://www.healthcare.philips.com/>) images were obtained to assess left ventricular end-diastolic dimension (LVEDd) and left ventricular end-systolic dimension (LVESd) at the midpapillary muscle level by a single-blinded observer. Two weeks after the transplantation, a similar echocardiogram was performed again. Left ventricular % fractional shortening (% FS), thickness of anterior wall, and thickness of posterior wall were calculated from 5–6 traces and averaged. Left ventricular pressure, brain natriuretic peptide (BNP), body weight, and heart weight (wet) were measured as previously described. Tissue samples were obtained by slicing along the short-axis of the left ventricle, for every 1 mm of depth. After masson trichrom staining, the area of fibrosis was digitized from

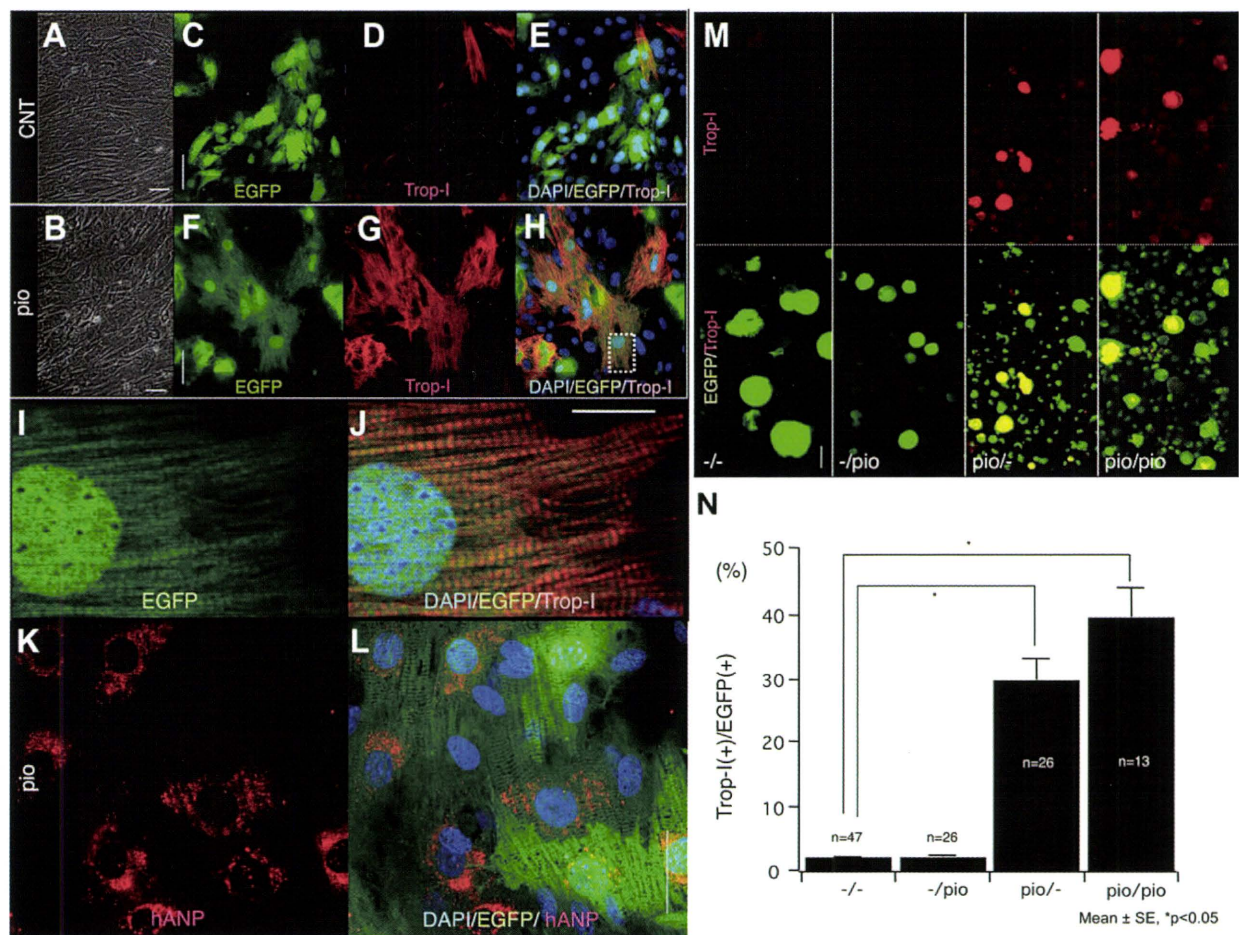


Figure 1. Pioglitazone improved CTE in vitro. Phase-contrast image of pio-administered marrow-derived mesenchymal stem cells ([B], pio) was not changed significantly compared with the default state ([A], CNT). Confocal microscopic images of immunocytochemistry after cardiomyogenic induction (coculture with murine cardiomyocytes) using anticardiac troponin-I (red; Trop-I) revealed significant augmentation of EGFP/Trop-I double-positive cardiomyocytes by pio (F–H), whereas EGFP/Trop-I double-positive cells were rare in CNT (C–E). Area within the dotted white box is expanded and shown in (I, J). Clear striation staining pattern of Trop-I was observed in every EGFP-positive cell. (K, L): Immunocytochemistry using human atrial natriuretic peptide (red; hANP), clear dot-like staining around nuclei observed in EGFP-positive cardiomyocytes. Please note striation pattern of EGFP intensity in (I, L). (M): Confocal microscopic image of immunocytochemistry (Trop-I) of isolated mesenchymal stem cells after cardiomyogenic induction. Condition of pretreatment of pio (before slash) and pio treatment after induction (after slash) are shown in the bottom. The calculated rate of Trop-I-positive cells in EGFP-positive cells are averaged and shown in (N). Pretreatment of pio increased the incidence of Trop-I-positive cells significantly. Scale bars = 50 μ m (A, B, C, F, M); 20 μ m (J). Abbreviations: CNT, control; DAPI, 4'-6-diamidino-2-phenylindole; EGFP, enhanced green fluorescent protein; pio, pioglitazone.

each slice, and then the % fibrosis volume in the left ventricular myocardium was calculated, as previously described [9]. Immunohistochemical analysis was performed using anti-rat CD34 antibody (1:200; R&D Systems, Minneapolis, MN, <http://www.rndsystems.com/>; AF4117) to evaluate vascular density. Then, biotinylated goat immunoglobulins (Dako, Carpinteria, CA, <http://www.dako.com/>; E0466) were used as a second antibody, next, strept ABC complex/Horseradish peroxidase (Dako; K0377), and finally, 3,3'-diaminobenzidine substrate (Wako; K3183500) was used. The images were digitized and the % brown pixel area of the capillary vessels was counted in the peri-infarct normal zone (Nz) and the center of the MI zone (MI) using a light microscope at $\times 10$ magnification. The area in five high-power fields was calculated and averaged.

Statistical Analysis

All data are shown as mean value \pm SE. The difference between mean values was determined with one-way analysis of variance (ANOVA) test or one-way repeated measures ANOVA test and Bonferroni post hoc test. Statistical significance was set at $p < .05$.

www.StemCells.com

RESULTS

Pretreatment with Pioglitazone Increased Efficiency of Cardiomyogenic Transdifferentiation via PPAR- γ Receptor Activation

Administration of pioglitazone did not cause any significant change in morphology of BM-MSCs (Fig. 1A, 1B), whereas improved CTE in vitro was observed. In this study, treatment with pioglitazone (pio) dramatically increased the incidence of beating BM-MSCs. Immunocytochemistry revealed a dramatic increase in incidence of cardiac troponin-I (Trop-I)/EGFP-double positive BM-MSCs in the pioglitazone-administrated experiment (Fig. 1F–1H), whereas the double-positive BM-MSCs were rare in the control (CNT) experiment (Fig. 1C–1E). The staining pattern of Trop-I showed a clear striation pattern in the differentiated BM-MSCs (Fig. 1I, 1J). EGFP and Trop-I-staining appeared alternately in a striated manner, suggesting that Trop-I was expressed in the cytoplasm of EGFP-positive cells. The transdifferentiated pioglitazone-treated BM-

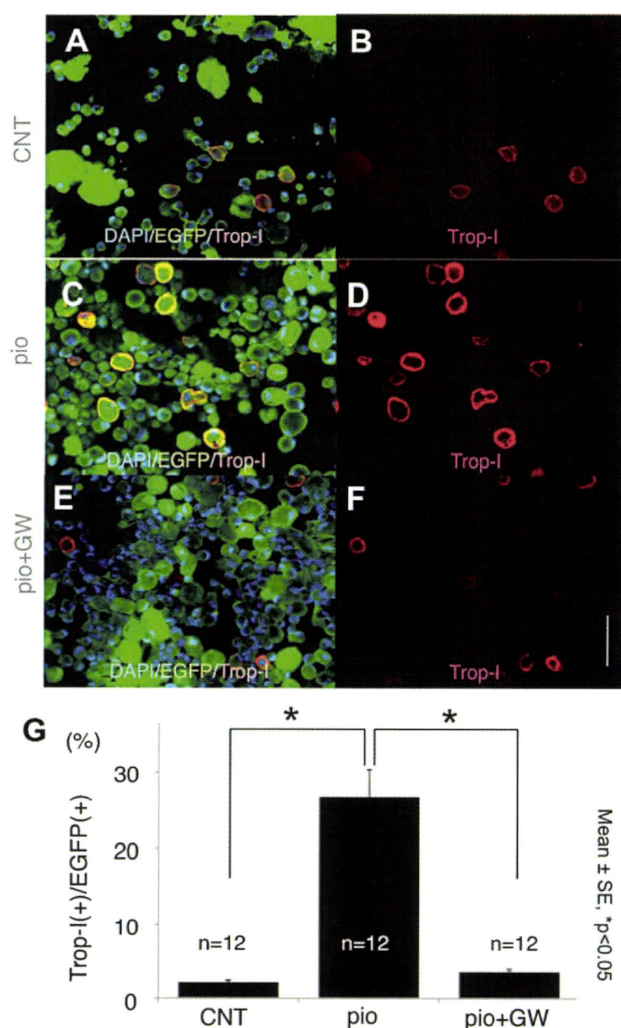


Figure 2. The effect of pioglitazone was mediated by peroxisome proliferator-activated receptor- γ activation. (A–F) Confocal microscopic image of immunocytochemistry (Trop-I) of isolated mesenchymal stem cells after cardiomyogenic induction. The rate of Trop-I positive cells in EGFP-positive cells was significantly increased by the pioglitazone treatment compared to non-treated cells (CNT) and the effect of pio was completely blocked by GW9662, as a specific blocker of peroxisome proliferator-activated receptor- γ . The calculated rate of Trop-I positive cells in EGFP-positive cells are averaged and shown in G. Scale bar denotes 50 μ m. Abbreviations: CNT, control; EGFP, enhanced green fluorescent protein; GW, GW9662; pio, pioglitazone; Trop-I, tropoin-I.

MSCs showed diffuse dot-like staining of hANP around the nuclei (Fig. 1K, 1L), clear striation pattern of sarcomeric α -actinin, and a diffuse dot-like staining pattern of Cx43 at the margin of the cells, whereas these did not show in the control BM-MSC experiment (supporting information Fig. 1). Similar pioglitazone-induced improvement in CTE was also observed in PCPCs and AMCs (data not shown).

To clarify the target of the pioglitazone, pioglitazone was administered only before the coculture or only after the coculture. Smear preparations of enzymatically isolated cells were stained with Trop-I (Fig. 1M) and CTE was calculated (Fig. 1N). Administration of pioglitazone after the start of coculture did not affect the CTE; on the other hand, pretreatment with pioglitazone significantly increased CTE (Fig. 1M). This suggests that pioglitazone modified the character of BM-MSCs to be able to cause higher CTE.

The effect of pioglitazone is known to be mediated by two nuclear receptors, PPAR- γ and retinoid X receptor [19]. In the present study, therefore, we use GW9662 as a specific PPAR- γ blocker to know which receptor is the essential one for this pioglitazone effect. The result showing that GW9662 completely blocked pioglitazone-induced increase in CTE in BM-MSCs (supporting information Fig. 2), suggests this effect is caused by a PPAR- γ -dependent pathway. PPAR- γ is the nuclear receptor, which regulates gene expressions and which might affect pioglitazone-induced increases in CTE. Therefore, gene chip analysis was performed to compare the expression pattern between control and pioglitazone-treated BM-MSCs. Consistently, upregulated genes and downregulated genes by the administration of pioglitazone in BM-MSCs are shown in supporting information Table 1 and supporting information Table 2, respectively.

Effect of PPAR- γ -Activated BM-MSC Transplantation on Cardiac Function In Vivo

The BM-MSCs were transplanted into the hearts of nude rats with chronic MI, in vivo, and the effect on cardiac function was examined. Before the cellular transplantation (2 weeks), there was no difference in the % FS (Fig. 2B) at the baseline. The difference in % FS (Δ % FS) at 2 weeks after transplantation is shown in Figure 2C. Oral administration of pioglitazone did not affect Δ % FS of MI model (CNT vs. CNT+po). Default BM-MSC transplantation also did not cause a significant effect (CNT vs. BM). On the other hand, pretreatment with pioglitazone significantly improved the efficacy of BM-MSC transplantation (BM vs. p-BM, BM+po vs. p-BM+po). Oral administration of pioglitazone, also significantly improved % FS in p-BM group (p-BM vs. p-BM+po). There was no difference in Δ LVEDd in any group (Fig. 2D) and significant decrease in Δ LVEDd of p-BM group compared with BM group (Fig. 2E). Thus, p-BM transplantation improved systolic function. It is also notable that the efficacy of default BM-MSC transplantation was significantly improved by oral administration of pioglitazone, suggesting that the effect of pioglitazone on BM-MSCs, to some extent, can be expected even after the transplantation. There was no difference in body weight (Fig. 3A), in serum BNP concentration (Fig. 3B), or other hemodynamic parameters (Fig. 3C–3F).

Heart weights were significantly increased by MI (Sham vs. CNT; Fig. 4A). The MI-induced increase in heart weight was blocked by orally administrated pioglitazone (CNT vs. CNT+po), and pioglitazone-pretreated BM-MSC transplantation (BM vs. p-BM). Left ventricular (LV) systolic pressure was significantly improved by pioglitazone-pretreated BM-MSCs (BM vs. p-BM; Fig. 4B). Orally administrated pioglitazone alone improved LV systolic pressure of CNT groups, whereas it did not improve echocardiographic parameters, suggesting that pioglitazone-induced water retention [20] might have played a role in this LV pressure to some extent.

The heart section was stained with masson-trichrome (Fig. 4C) and the fibrosis volume was measured and averaged (Fig. 4D). The % fibrosis volume was significantly decreased by p-BM transplantation compared with BM.

Mechanism for Recovery in Cardiac Functions

ELISA analysis revealed default BM-MSCs significantly secrete angiogenesis-related molecules, that is, angiotensin-II, bFGF, HB-EGF, HGF, leptin, PIGF, and VEGF in the culture medium, and they were not changed by pioglitazone administration (Fig. 5). Concordant with this result (Fig. 6G), at the MI area, BM transplantation significantly increased the vessel density at the center of the MI area (CNT vs. BM), but there

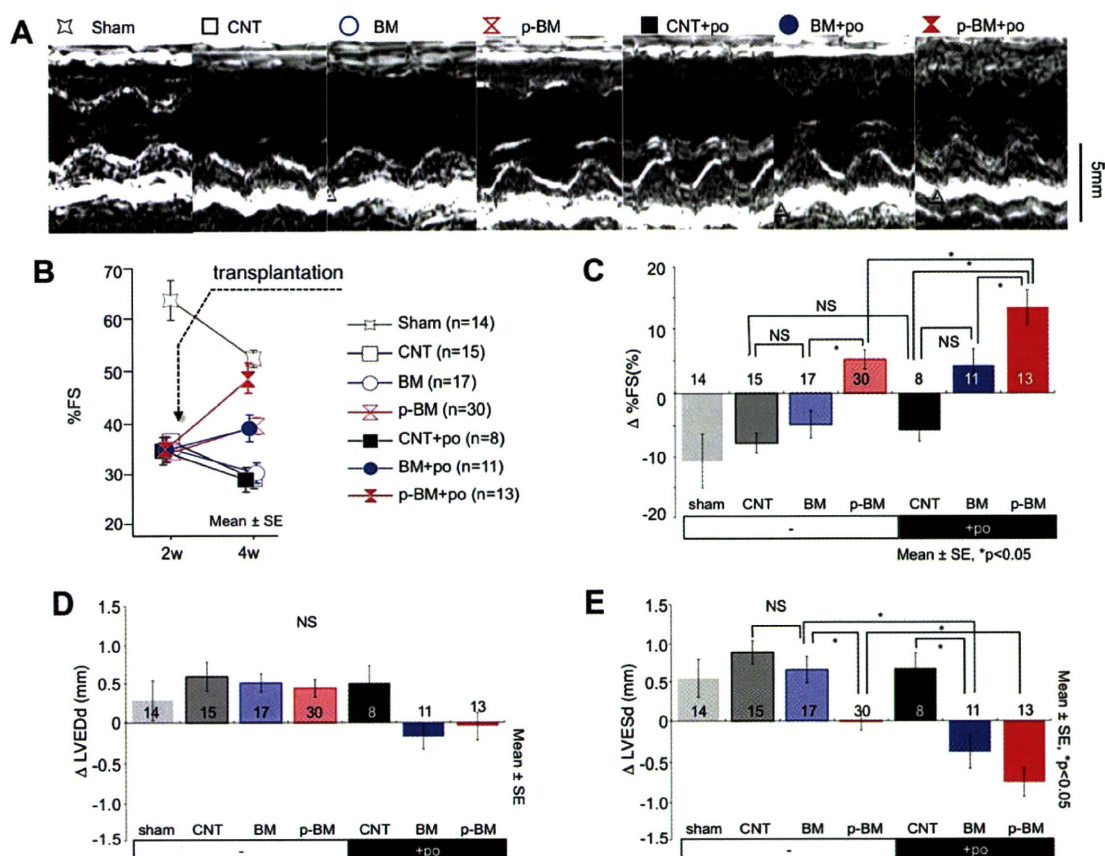


Figure 3. Effect of pioglitazone-pretreated bone marrow-derived mesenchymal stem cell (BM-MSC) transplantation and/or oral administration of pioglitazone on echocardiographic parameters in vivo. (A): Representative trace of M-mode echocardiogram from the Sham-operated nude rats, control myocardial infarction (CNT), myocardial infarction with BM-MSCs transplantation (BM), pioglitazone-pretreated BM (p-BM), and additional oral administration of pioglitazone after the transplantation (CNT+po, BM+po, p-BM+po) are shown. (B): Calculated left ventricular % fractional shortening (% FS) from each group at 2 weeks after the first operation (immediately before transplantation) and 4 weeks after the first operation are shown. There was no difference in % FS at 2 weeks; however, p-BM, BM+po, and p-BM+po significantly improved % FS after cellular transplantation (4 weeks). Change in % FS from 2 to 4 weeks ([C], Δ% FS), left ventricular end diastolic dimension ([D], ΔLVEDd), and left ventricular end systolic dimension ([E], ΔLVESd) are averaged and shown. Abbreviations: CNT, control; DAPI, 4'-6-diamidino-2-phenylindole; EGFP, enhanced green fluorescent protein; GW, GW9662; pio, pioglitazone.

was no statistical significance between BM versus p-BM. On the other hand, orally administrated pioglitazone significantly increased the vessel density at the peri-MI normal area (Nz, CNT vs. CNT+po), and additionally increased the vessel density at the center of the MI area of p-BM groups (Nz, p-BM vs. -BM+po). This angiogenic effect was also observed independent of BM-MSC transplantation, suggesting that the effect was partially caused by pioglitazone-induced VEGF-expression in vascular smooth muscle [21].

Immunohistochemical analysis was performed to observe the fate of EGFP-labeled BM-MSCs in situ. In the BM group and the BM+po group, there were many EGFP-positive cells in the MI area; however, these cells were enucleated and there were no EGFP/Trop-I double-positive cardiomyocytes (Fig. 7A). In the p-BM group, there were a lot of EGFP-positive cells in the MI area (Fig. 7B), and sometimes we observed EGFP-negative/Trop-I positive cells adjacent to the EGFP-positive cells (Fig. 7C), which may represent p-BM-induced survival of host cardiomyocytes in the MI zone, which may be due to an augmented paracrine effect of p-BM. Surprisingly, in the p-BM+po group, the survival rate of EGFP/Trop-I double-positive cells are significantly increased (Fig. 7I) and there were many EGFP/Trop-I double-positive

cells at the border zone of the MI (Fig. 7D, arrows) that showed a clear striation staining pattern of Trop-I (Fig. 7E). Many EGFP/sarcomeric α -actinin double-positive cardiomyocytes were also observed (Fig. 7F) that showed a clear striation staining pattern (Fig. 7G). Furthermore, there was band-like staining of Cx43 expression at the margin of the EGFP-positive cardiomyocytes to the host cardiomyocytes (Fig. 7G), suggesting tight electrical coupling. The α -actinin and EGFP staining were observed alternately in a striated manner (*), suggesting that α -actinin is expressed in the EGFP-positive cells (Fig. 7H). In the p-BM+po group, cardiomyocytes were enzymatically isolated and EGFP-positive rod-shaped cardiomyocytes (striation was observed by phase-contrast image, supporting information Fig. 3A, 3B) and EGFP-negative rods were selected; then, the fluorescence in situ hybridization experiment was performed. The EGFP-negative rods were negative for human-specific Alu and positive for Rat-X chromosome (supporting information Fig. 3C–3F). On the other hand, EGFP-positive rods were positive for human-specific Alu, whereas negative for Rat-X (supporting information Fig. 3G–3J), suggesting that EGFP-positive cardiomyocytes were derived from human BM-MSCs not by cell fusion but by cardiomyogenic transdifferentiation.

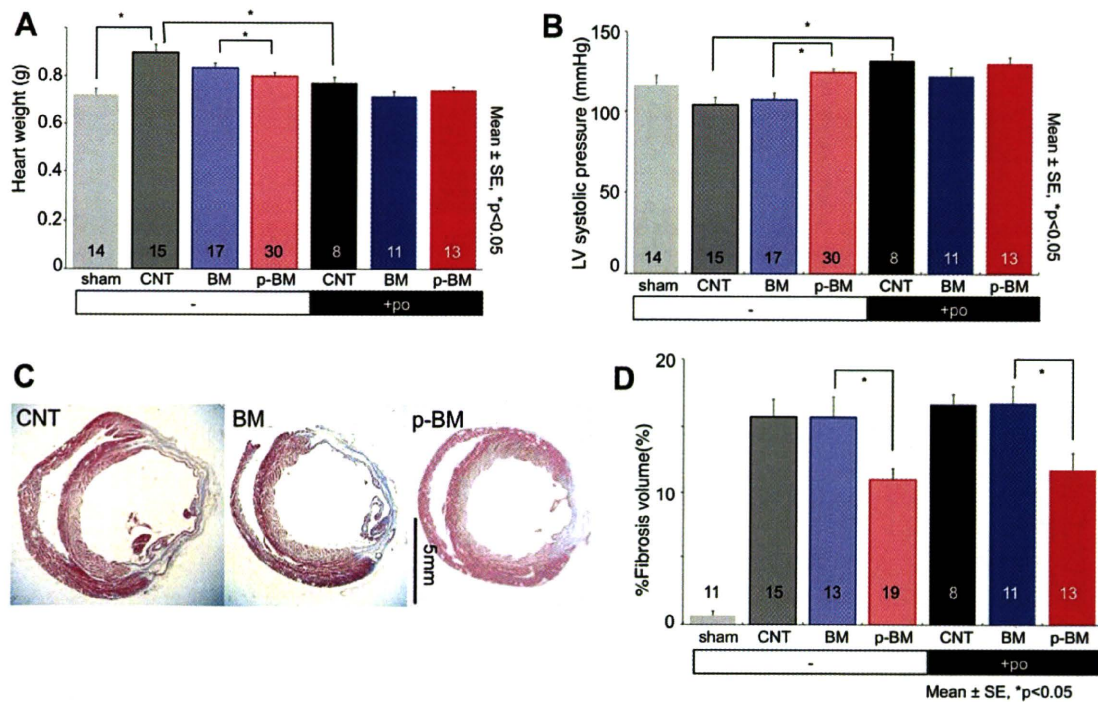


Figure 4. Effect of pioglitazone-pretreated bone marrow-derived mesenchymal stem cells (BM-MSCs) transplantation and/or oral administration of pioglitazone on hemodynamic parameters and infarction size in vivo. (A): Wet heart weight, (B) left ventricular systolic pressure (LVSP), and (C) % fibrosis volume of left ventricle from each group at 4 weeks after the first operation. Sham-operated nude rats, control myocardial infarction (CNT), myocardial infarction (MI) with BM, p-BM, and additional oral administration of pioglitazone after the transplantation (CNT+po, BM+po, p-BM+po) are averaged and shown. Oral administration of pioglitazone significantly improved MI-induced cardiac hypertrophy (A) and MI-induced deterioration of LVSP (B). The effect of pio was also observed only by pretreatment with BM-MSCs and without oral administration. Representative masson-trichrom staining of the heart at the tendinous cord level of CNT, BM, and p-BM are shown. The digitized data were measured and calculated in (D). By the pio-pretreatment, BM-MSCs transplantation significantly decreased in % fibrosis volume. Scale bar = 5 mm. Abbreviations: BM, bone marrow-derived mesenchymal stem cells transplantation; CNT, control; LV, left ventricular; p-BM, pioglitazone-pretreated BM, pio, pioglitazone.

DISCUSSION

In this study, pioglitazone dramatically increased the CTE of human BM-MSCs via PPAR- γ activation in vivo and in vitro. Pioglitazone-pretreated BM-MSC transplantation significantly improved impaired cardiac function in the MI model in vivo and significantly reduced % volume of the MI. Orally administered pioglitazone significantly improved cardiac function further when BM-MSCs were transplanted, and significantly improved the survival of BM-MSC-derived cardiomyocytes in vivo.

The Mechanisms of Improvement in CTE by PPAR- γ Activation

Pioglitazone, a major antidiabetic agent, enhances adipocyte differentiation via PPAR- γ activation [22] and secretion of adiponectin [23], and improves insulin sensitivity in patients with type II diabetes mellitus [24]. The endogenous agonist for PPAR- γ receptor is 15-deoxy- Δ (12,14)-prostaglandin J_2 (15d-PG J_2), an end product of arachidonic acid and prostaglandin D $_2$. As, PPAR- γ abundantly distributes in adipose tissue, the main target has been believed to be adipose tissue; however, PPAR- γ is known to be expressed in mesenchymal cells [25], and PPAR- γ activation changed the phenotype of mesenchymal cells during cardiomyogenesis. In the present study, we concluded that pioglitazone-induced increase in transdifferentiation was caused by PPAR- γ , because it was completely

blocked by GW9662, a specific PPAR- γ blocker. The favorable effect on CTE was observed by rosiglitazone (1 μ mol/l, 37.0% \pm 2.9% n = 20), also suggesting the class effect.

It is notable that neither administration of pioglitazone alone (without cocultivation) nor administration of pioglitazone after the onset of cocultivation caused cardiomyogenic transdifferentiation. These data suggest that pioglitazone did not directly induce the cardiomyogenic transdifferentiation or augment the effect of cardiomyogenic transdifferentiating humoral factors derived from murine cardiomyocytes. In our pilot study, pretreatment with pioglitazone for 2 days before the start of cocultivation did not cause any improvement in efficiency, suggesting the slow effect of pioglitazone. From these observations, we concluded that pretreatment with pioglitazone changed the cellular biology of the MSC and we, therefore, called this state a "potentiation of cells," in the present study, but precise molecular mechanisms remain elucidated.

Furthermore, mechanisms of cardiomyogenic "transdifferentiation" are also unclear. Our previously reported AMCs [26], UCB-MSCs [8], MMCs, and endometrial gland-derived mesenchymal cells (EMCs) [9] might be referred to as "potentiated cells." Despite this potentiated cells express almost all cardiomyocytes-specific genes, that is, Nkx 2.5, GATA-4, cardiac troponin-I. at the default state [8–10], however, they did not spontaneously transdifferentiate into cardiomyocytes. Therefore, we speculated that some epigenetic stimulation or cell-to-cell communication may play an important role in causing cardiomyogenic transdifferentiation of the MSCs.

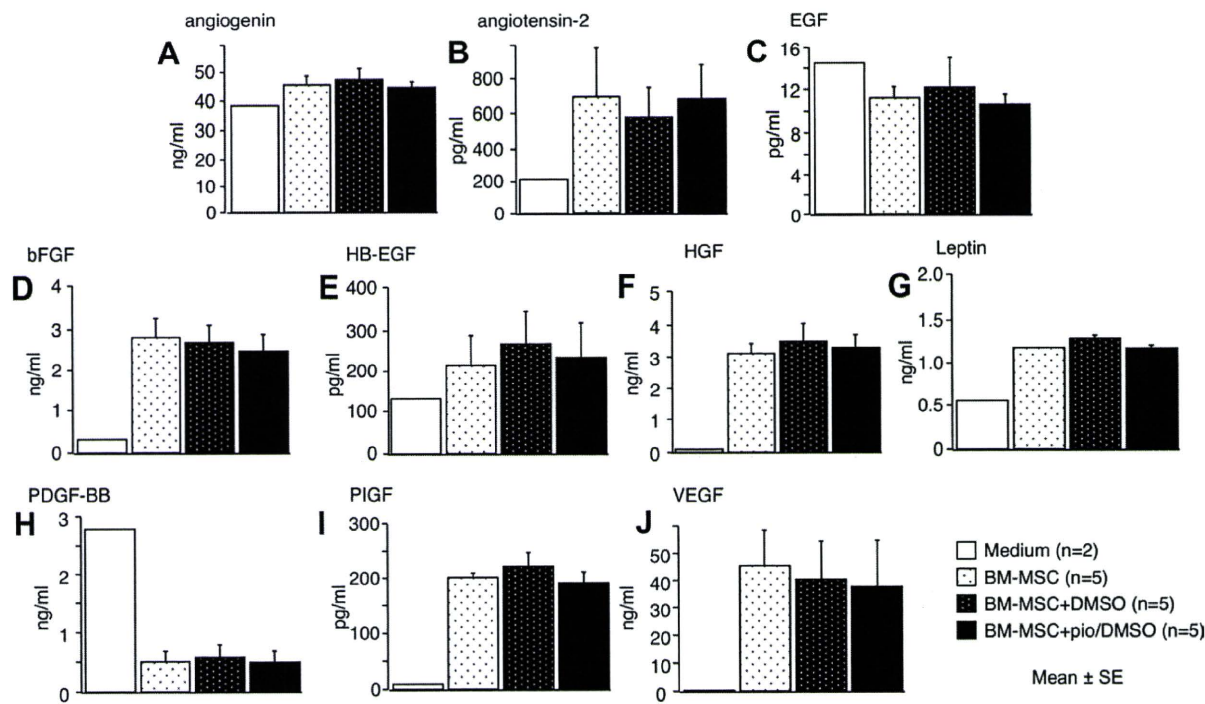


Figure 5. Secretion of angiogenic humoral factors from bone marrow-derived mesenchymal stem cells into the culture medium supernatant and the effect of pioglitazone in vitro. Concentration of angiogenic humoral factors (angiogenin [A], angiotensin-2 [B], EGF [C], bFGF [D], HB-EGF [E], HGF [F], leptin [G], PDGF-BB [H], PIGF [I], VEGF [J]) in culture medium was measured by enzyme-linked immunosorbent assay and averaged. Pioglitazone treatment did not cause any change. Abbreviations: bFGF, basic fibroblast growth factor; BM, bone marrow; DMSO, dimethyl sulfoxide; EGF, epidermal growth factor; HB-EGF, heparin-binding EGF-like growth factor; HGF, hepatocyte growth factor; MSC, mesenchymal stem cell; PDGF-BB, platelet-derived growth factor-BB; PIGF, phosphatidylinositol-glycan biosynthesis class F protein; VEGF, vascular endothelial growth factor.

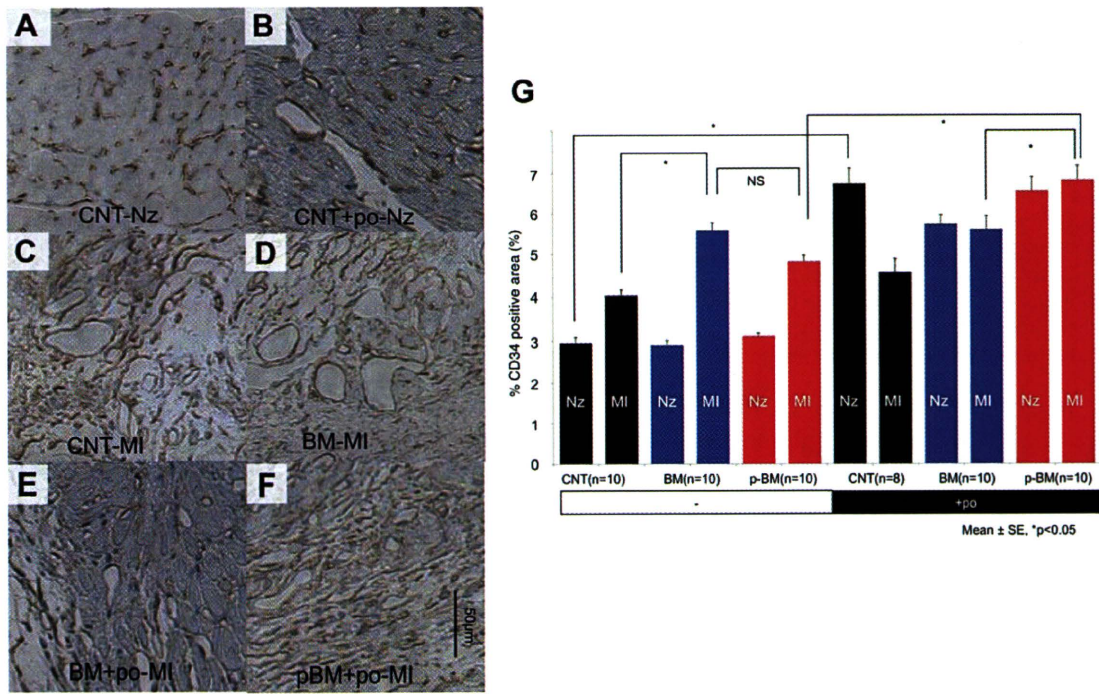


Figure 6. Effect of bone marrow-derived mesenchymal stem cells transplantation and/or treatment with pioglitazone on vessel density in the heart in vivo. (A–F): Representative microscopic image of immunohistochemistry using anti-CD34 antibody to detect vessels at center of MI zone and peri-MI normal zone are shown. Scale bar = 50 μ m. (G): The % CD34-positive area in control myocardial infarction (CNT), MI with BM, p-BM, and additional oral administration of pioglitazone after the transplantation (CNT+po, BM+po, p-BM+po) are calculated and averaged. Abbreviations: BM, bone marrow-derived mesenchymal stem cells transplantation; CNT, control; MI, myocardial infarction; Nz, normal zone; NS, not statistically significant; p-BM, pioglitazone-pretreated BM.

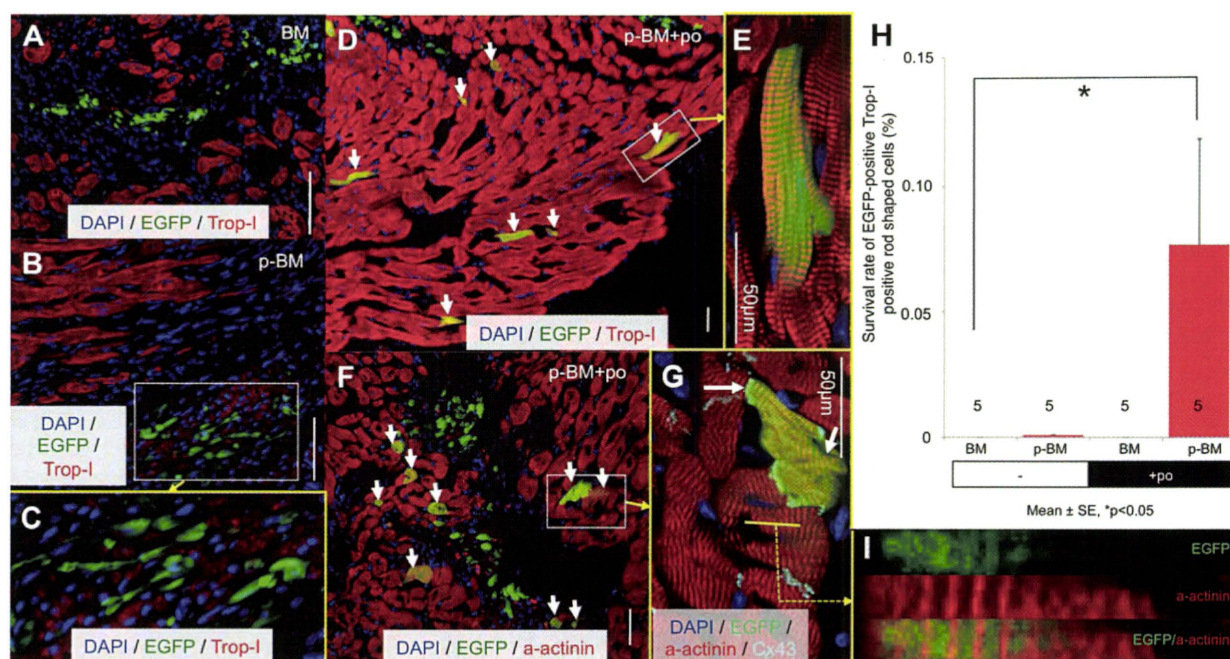


Figure 7. Oral administration of pioglitazone significantly improved the incidence of survival of pioglitazone-pretreated bone marrow-derived mesenchymal stem cells (BM-MSCs)-derived cardiomyocytes in vivo. Confocal laser microscopic image of immunohistochemistry using anti-cardiac troponin-I antibody (red; Trop-I) are shown. (A): After transplantation of default BM-MSCs (BM), EGFP-positive (green) cells can be observed at the margin of the myocardial infarction (MI), but there were no EGFP/Trop-I double-positive cardiomyocytes. Almost all EGFP-positive cells are enucleated at MI area. (B): After transplantation of p-BM, EGFP-positive cells can be observed around the Trop-I-positive host cells; however, EGFP/Trop-I-double positive cells were rare ([C], expanded image at the white box in [B]). (D): After transplantation of p-BM and oral administration of pioglitazone (p-BM+po), many EGFP/Trop-I-positive cells surviving at the peri MI zone (white arrow). A representative image of rod-shaped cells is expanded and shown in panel [E] (corresponding to the white box in panel [D]). A clear striation pattern of Trop-I and also striation of EGFP were observed. (F): Many EGFP/ α -actinin double-positive cells were observed (white arrow) around the needle hole. An expanded image at the white box in panel (F) is shown in (G). (G): A clear connexin 43 (Cx43) stain was observed at the margin of the EGFP/ α -actinin double-positive cells. The striation staining pattern at the yellow line of panel (G) is shown in panel (H). The α -actinin and EGFP staining was observed alternately in a striated manner (*), suggesting α -actinin is expressed in the EGFP-positive cell. (I): The percentage of EGFP/Trop-I-double positive rod-shaped cells in the injected EGFP-positive cells were averaged and shown. In the p-BM+po group, a significant number of EGFP/Trop-I double-positive rod-shaped cells survived. Scale bars = 50 μ m (A, B, D, E, F, G). Abbreviations: BM, bone marrow-derived mesenchymal stem cells transplantation; DAPI, 4'-6-diamidino-2-phenylindole; EGFP, enhanced green fluorescent protein; p-BM, pioglitazone-pretreated MSCs.

The Effect of Orally Administrated Pioglitazone in Cardiac Functions of MI Model

The orally administrated pioglitazone alone significantly reduced MI-induced cardiac hypertrophy and LV systolic pressure, and did not affect other hemodynamic parameters. Therefore, the effect on LV pressure may be caused in part by pioglitazone-induced fluid retention [20]. Despite increased vascular density at the peri-MI by pioglitazone administration, % fibrosis volume was not changed; therefore, this angiogenic effect could not help reduce % fibrosis volume, in the present study. Shiomi et al. [27] clearly showed that the oral administration of pioglitazone significantly improved left ventricular systolic functions in the acute MI model; however, in the chronic MI model [28], the effect of pioglitazone could not be observed. Thus, we concluded that orally administrated pioglitazone alone did not cause any improvement of ventricular systolic functions in the chronic MI model and the beneficial effect was observed only when the BM-MSCs were transplanted, suggesting that the effects are mediated by BM-MSCs.

The Effect of Pioglitazone-Pretreated Human Marrow-Derived MSCs on Cardiac Functions In Vivo

In this study, BM-MSCs slightly improved $\Delta\%$ FS, but there was no statistical significance. On the other hand, pretreat-

ment with pioglitazone of BM-MSCs significantly improved $\Delta\%$ FS, Δ LVESd, LV systolic pressure, % fibrosis volume, and normalized post MI-induced hypertrophy of heart weight. As the number of surviving BM-MSC-derived cardiomyocytes was rare, the improvement in cardiac function may not be due to newly generated cardiomyocytes. Pioglitazone pretreatment did not affect secretion of angiogenic factors in vitro and vessel density in vivo; thus, the effect of the pioglitazone on cardiac function may not be caused by the angiogenesis. We speculated that the potentiated BM-MSCs might increase secretion of unspecified factors, which may be contributing antiapoptotic action to the host myocardium [12] or suppressing post MI left ventricular remodeling.

Our data showed that the effect of "human" BM-MSCs at the default state on cardiac function was low. The discrepancy from a previous experimental report [29] performed by "nonhuman" BM-MSCs might be due to low angiogenic effect or low paracrine effect of "human cells." From another aspect, our data of default human BM-MSCs can explain the poor efficacy of BM-MSC in the clinical reports [30]. Such poor efficacy might be due to low angiogenic and/or paracrine effect of "human" BM-MSCs. Therefore, if we potentiate BM-MSCs by means of pioglitazone, we may be able to expand the efficacy of BM-MSCs in the clinical study.

Comparison of Mesenchymal Cells with Other Organs

In contrast to other mesenchymal cells, BM-MSCs can be used as an autograft and have been transplanted into a clinical patient [31]; therefore, BM-MSCs are ready to use and are still an important candidate as a cardiac stem cell source. On the other hand, CTE of BM-MSCs at the default state was far less than other mesenchymal cells, that is, MMC [9], AMC [11], UCB-MSC [8]. In this study, pretreatment with pioglitazone dramatically improved the CTE of BM-MSCs in vitro. We suspected that the difference in CTE of mesenchymal cells obtained from various organs might be due to different degrees of stimulation with intrinsic 15d-PGJ₂ of each mesenchymal cell at the default state. But in our preliminary observation, pretreatment with GW9662 did not suppress the CTE of MMCs and EMCs; therefore, the precise mechanism of different CTE of mesenchymal cells at the default state is still unclear.

Study Limitations

From the in vivo experiment, we feel the number of surviving BM-MSC-derived cardiomyocytes is not enough for restoring impaired cardiac function, at this time. But taking into account the extremely low CTE in the previous article [5, 13], it is a great advance that such a significant number of human BM-MSCs can be transdifferentiated into cardiomyocytes in vivo by use of pioglitazone. Our experimental model might provide us with a first clue as to the adequate BM-MSC-transplantation methods that can be expected to show dramatic cardiomyogenesis in vivo. Further experimentation should be done.

From another point of view, the beneficial effect of pioglitazone on cardiac function might be caused by augmentation of a paracrine effect of BM-MSCs. In this study, precise mechanisms for a paracrine effect were not yet determined, as it may be caused by unknown molecules and/or may be caused by a cell-mediated mechanism (i.e., immune cells). The precise molecular or cellular mechanism should be elucidated in the near future.

For the in vitro experiment, pioglitazone pretreatment before cardiomyogenic induction was necessary and was shown to be a sufficient condition for dramatic improvement of cardiomyogenic transdifferentiation. In contrast, not only pretreatment with pioglitazone but also additional oral administration of pioglitazone was essential to observe a significant number of surviving BM-MSC-derived cardiomyocytes in vivo. The apparently different results between in vitro and in vivo may be

explained by a significant loss in the number of transplanted BM-MSCs that might have occurred in the in vivo condition, that is, apoptosis, and that might have been improved by orally administered pioglitazone. The orally administered pioglitazone-induced angiogenic effect at peri-MI normal zone and/or antiapoptotic effect [32] might be essential for the survival of transdifferentiated cardiomyocytes. Improvement of survival of BM-MSCs in situ might also improve the effect of transplantation of BM-MSCs in this study.

In this study, BM-MSCs were obtained from a single donor. However, the same effect of pioglitazone was observed in BM-MSCs from neonate and PCPCs [10], AMCs [26] in our pilot study, suggesting that the effect of pioglitazone can be applied generally to human mesenchymal cells.

The fluorescent intensity of EGFP significantly decreases around 2 weeks after the transfection [26]; therefore, we examined cardiac function and performed the histological experiment at 2 weeks after the transplantation, in the present study. The durability of the preferable effect of pioglitazone-treated BM-MSC transplantation for more than 2 weeks was unclear.

CONCLUSION

Not only improvement of cardiomyogenic transdifferentiation efficiency but also improvement of paracrine action of BM-MSCs was elicited by pretreatment with pioglitazone. Pioglitazone is a popular medicine, and clinical application of transplantation of BM-MSCs for hearts has already been done; therefore, our proposed method is a ready-to-use method. Cardiac stem cell therapy by autologous BM-MSC transplantation can improve the efficacy and expected cardiomyogenic transdifferentiation by pioglitazone treatment. Pioglitazone-pretreated BM-MSC transplantation can be a promising cardiac stem cell therapy and may dramatically advance the modest efficacy of stem cell therapy at the present time.

ACKNOWLEDGMENTS

The research was partially supported by a grant from the Ministry of Education, Science and Culture, Japan. A part of this work was undertaken at the Keio Integrated Medical Research Center.

REFERENCES

- Boheler KR, Czyz J, Tweedie D et al. Differentiation of pluripotent embryonic stem cells into cardiomyocytes. *Circ Res* 2002;91:189–201.
- Okita K, Ichisaka T, Yamanaka S. Generation of germline-competent induced pluripotent stem cells. *Nature* 2007;448:313–317.
- Andrews PW. From teratocarcinomas to embryonic stem cells. *Philos Trans R Soc Lond B Biol Sci* 2002;357:405–417.
- Masaki H, Ishikawa T, Takahashi S et al. Heterogeneity of pluripotent marker gene expression in colonies generated in human iPS cell induction culture. *Stem Cell Res* 2007;1:105–115.
- Takeda Y, Mori T, Imabayashi H et al. Can the life span of human marrow stromal cells be prolonged by bmi-1, E6, E7, and/or telomerase without affecting cardiomyogenic differentiation? *J Gene Med* 2004;6:833–845.
- Beltrami A, Barlucchi L, Torella D et al. Adult cardiac stem cells are multipotent and support myocardial regeneration. *Cell* 2003;114:763–776.
- Tateishi K, Ashihara E, Honsho S et al. Human cardiac stem cells exhibit mesenchymal features and are maintained through Akt/GSK-3beta signaling. *Biochem Biophys Res Commun* 2007;352:635–641.
- Nishiyama N, Miyoshi S, Hida N et al. The significant cardiomyogenic potential of human umbilical cord blood-derived mesenchymal stem cells in vitro. *Stem Cells* 2007;25:2017–2024.
- Hida N, Nishiyama N, Miyoshi S et al. Novel cardiac precursor-like cells from human menstrual blood-derived mesenchymal cells. *Stem Cells* 2008;26:1695–1704.
- Okamoto K, Miyoshi S, Toyoda M et al. 'Working' cardiomyocytes exhibiting plateau action potentials from human placenta-derived extraembryonic mesodermal cells. *Exp Cell Res* 2007;313:2550–2562.
- Tsuji H, Miyoshi S, Ikegami Y, et al. Xenografted human amniotic membrane-derived mesenchymal stem cells are immunologically tolerated and transdifferentiated into cardiomyocytes. *Circ Res* 2010;106:1613–1623.
- Gnecchi M, He H, Liang O et al. Paracrine action accounts for marked protection of ischemic heart by Akt-modified mesenchymal stem cells. *Nat Med* 2005;11:367–368.
- Gojo S, Gojo N, Takeda Y et al. In vivo cardiovascularogenesis by direct injection of isolated adult mesenchymal stem cells. *Exp Cell Res* 2003;288:51–59.
- Kocher AA, Schuster MD, Szabolcs MJ et al. Neovascularization of ischemic myocardium by human bone-marrow-derived angioblasts prevents cardiomyocyte apoptosis, reduces remodeling and improves cardiac function. *Nat Med* 2001;7:430–436.

- 15 Ikegami Y, Miyoshi S, Nishiyama N et al. Serum-independent cardiomyogenic transdifferentiation in human endometrium-derived mesenchymal cells. *Artif Organs* 2010 (in press).
- 16 Gilbertson JR. *Cardiac Muscle in Lipid Metabolism in Mammals*. Vol. 1. New York: Plenum Press, 1977.
- 17 Puigserver P, Spiegelman BM. Peroxisome proliferator-activated receptor- γ coactivator 1 α (PGC-1 α): Transcriptional coactivator and metabolic regulator. *Endocr Rev* 2003;24:78–90.
- 18 Matsuura K, Wada H, Nagai T et al. Cardiomyocytes fuse with surrounding noncardiomyocytes and reenter the cell cycle. *J Cell Biol* 2004;167:351–363.
- 19 Kliewer SA, Umesono K, Noonan DJ et al. Convergence of 9-cis retinoic acid and peroxisome proliferator signalling pathways through heterodimer formation of their receptors. *Nature* 1992;358:771–774.
- 20 Tang WH, Francis GS, Hoogwerf BJ et al. Fluid retention after initiation of thiazolidinedione therapy in diabetic patients with established chronic heart failure. *J Am Coll Cardiol* 2003;41:1394–1398.
- 21 Yamakawa K, Hosoi M, Koyama H et al. Peroxisome proliferator-activated receptor- γ agonists increase vascular endothelial growth factor expression in human vascular smooth muscle cells. *Biochem Biophys Res Commun* 2000;271:571–574.
- 22 Yamauchi T, Kamon J, Waki H et al. The mechanisms by which both heterozygous peroxisome proliferator-activated receptor γ (PPAR γ) deficiency and PPAR γ agonist improve insulin resistance. *J Biol Chem* 2001;276:41245–41254.
- 23 Iwaki M, Matsuda M, Maeda N et al. Induction of adiponectin, a fat-derived antidiabetic and antiatherogenic factor, by nuclear receptors. *Diabetes* 2003;52:1655–1663.
- 24 Kadowaki T. Insights into insulin resistance and type 2 diabetes from knockout mouse models. *J Clin Invest* 2000;106:459–465.
- 25 Matsushita K, Wu Y, Okamoto Y et al. Local renin angiotensin expression regulates human mesenchymal stem cell differentiation to adipocytes. *Hypertension* 2006;48:1095–1102.
- 26 Tsuji H, Miyoshi S, Ikegami Y et al. Xenografted human amniotic membrane-derived mesenchymal stem cells are immunologically tolerated and transdifferentiated into cardiomyocytes. *Circ Res* 2010;106:1613–1623.
- 27 Shiomi T, Tsutsui H, Hayashidani S et al. Pioglitazone, a peroxisome proliferator-activated receptor- γ agonist, attenuates left ventricular remodeling and failure after experimental myocardial infarction. *Circulation* 2002;106:3126–3132.
- 28 Frantz S, Hu K, Widder J et al. Peroxisome proliferator activated-receptor agonism and left ventricular remodeling in mice with chronic myocardial infarction. *Br J Pharmacol* 2004;141:9–14.
- 29 Shake JG, Gruber PJ, Baumgartner WA et al. Mesenchymal stem cell implantation in a swine myocardial infarct model: Engraftment and functional effects. *Ann Thorac Surg* 2002;73:1919–1925; discussion: 1926.
- 30 Hare JM, Traverse JH, Henry TD et al. A randomized, double-blind, placebo-controlled, dose-escalation study of intravenous adult human mesenchymal stem cells (prochymal) after acute myocardial infarction. *J Am Coll Cardiol* 2009;54:2277–2286.
- 31 Chen SL, Fang WW, Ye F et al. Effect on left ventricular function of intracoronary transplantation of autologous bone marrow mesenchymal stem cell in patients with acute myocardial infarction. *Am J Cardiol* 2004;94:92–95.
- 32 Li J, Lang MJ, Mao XB et al. Antiapoptosis and mitochondrial effect of pioglitazone preconditioning in the ischemic/reperfused heart of rat. *Cardiovasc Drugs Ther* 2008;22:283–291.



See www.StemCells.com for supporting information available online.

Safety and efficacy of pericardial endoscopy by percutaneous subxyphoid approach in swine heart in vivo

Takehiro Kimura, MD,^a Shunichiro Miyoshi, MD, PhD,^a Seiji Takatsuki, MD, PhD,^a Kojiro Tanimoto, MD, PhD,^a Kotaro Fukumoto, MD, PhD,^a Kyoko Soejima, MD, PhD,^b and Keiichi Fukuda, MD, PhD^a

Objective: A nonsurgical approach from the epicardial surface is useful for various cardiac interventions, such as positioning of the left ventricular lead for cardiac resynchronization therapy and epicardial ablation. Stem cell delivery on the epicardial surface can be considered in the future if good quality of visualization can be obtained. However, because the pericardial space is limited, hemodynamic conditions may deteriorate with pericardial endoscopy. Therefore, the feasibility and efficacy of pericardial endoscopy were examined by using ready-made endoscopes.

Methods: Anesthetized swines (26–61 kg; n = 6) were used for the experiment. Electrocardiogram, femoral artery blood pressure, and oxygen saturation by pulse oximetry were continuously monitored during the procedures. Guided by the fluoroscopy, sheaths were advanced to the pericardial space using the modified Seldinger technique from the subxyphoid space.

Results: After insertion of an endoscope with a maximum diameter of 6.9 mm, hemodynamic parameters were stable during the procedure with atropine. Stable and acceptable endoscopic images were obtained. Minor operations can be performed with pericardial endoscopic-guided laparoscopic forceps with no complications.

Conclusions: The endoscopic pericardial procedure is effective and feasible. This procedure can increase the possibility and efficacy of nonsurgical treatment for cardiac diseases. (*J Thorac Cardiovasc Surg* 2010; ■:1-10)



Video clip is available online.

Recent progress in minimally invasive therapy has dramatically changed the treatment of heart disease. Percutaneous transluminal approaches (eg, coronary angioplasty¹; catheter ablation^{2,3}; pacemaker, implantable cardioverter defibrillator, and cardiac resynchronization therapy⁴; and percutaneous heart valve replacement⁵) have provided significant therapeutic benefit to patients with a minimal burden. However, it is still difficult to reach the epicardial targets by the transluminal approach. Minimally invasive epicardial approaches may aid epicardial biopsy, implantation of left ventricular epicardial pacing lead for cardiac resynchroniza-

tion therapy, and ablation for epicardial arrhythmic substrate. Furthermore, such approaches are also applicable for transplantation of stem cells into the myocardium. Although significant progress in research for cardiac stem cells has been made, research for optimization of the transplantation procedures is sparse. Compared with catheter-based transluminal stem cell transplantation,⁶ epicardial transplantation poses less risk for infusion of stem cells into the bloodstream and systemic dissemination and micro-embolization of overflowed stem cells.^{7,8} Pericardial endoscopy is also applicable to direct genetic transfection of the gene to the local myocardium, so-called gene therapy.⁹

Pericardiocentesis using the Seldinger maneuver from the subxyphoid to the pericardial space without obvious pericardial effusions is safe¹⁰ and allows the epicardial target to be reached with minimal invasion.^{11,12} However, it is difficult to perform the operation within the pericardial space because of numerous obstacles: the coronary vessels, adipose tissue, lung, and phrenic nerves. Therefore, endoscopic guidance is required for the operation. Epicardial biopsy,^{13,14} epicardial ablation,¹⁵ pulmonary vein isolation,¹⁶ and implantable cardioverter defibrillator lead placement¹⁷ using pericardial endoscopy have been reported, but risk of injury to arteries, organs, and nerves still remains. The relation among the diameter of the endoscope, material of the sheath, and hemodynamic parameters has not been extensively described. Epicardial inflammation as a chronic effect should be further evaluated. Techniques to obtain a more refined view for critical procedures are not well developed.

From Cardiology,^a Keio University School of Medicine, Tokyo Japan; and Cardiology,^b St. Marianna University School of Medicine, Kawasaki, Japan.

Experiments were partially supported by the Japanese Society for Promotion of Science, Grant-in-Aid for Scientific Research, the Ministry of Health, Labor, and Welfare of Japan, and the Suntory Fund for Advanced Cardiac Therapeutics, Keio University School of Medicine. Part of the work was performed at the Keio Research Laboratory Center for Integrated Medical Research.

Disclosures: None.

Received for publication Aug 1, 2010; revisions received Sept 5, 2010; accepted for publication Sept 11, 2010.

Address for reprints: Takehiro Kimura, MD, 35 Shinanomachi Shinjuku-ku Tokyo, Japan 160-8582, Cardiology, Keio University School of Medicine (E-mail: veritas@bp.ij4u.or.jp).

0022-5223/\$36.00

Copyright © 2010 by The American Association for Thoracic Surgery

doi:10.1016/j.jtcvs.2010.09.050

Abbreviation and Acronym

CCD = charge-coupled device

Therefore, we evaluated the safety of this procedure, not only for short time periods to assess hemodynamic changes but also for longer periods to assess chronic complications, including infections, chronic pericarditis, and other life-threatening complications. Among various ready-made endoscopes, adequate types for pericardial endoscopy were selected. To identify the anatomy of the heart, we defined the basic method to steer the endoscope and stabilize the view.

MATERIALS AND METHODS**Surgical Procedure**

All experimental protocols were approved by the institutional ethical committee. Studies were performed in 6 mongrel swine weighing 26 to 61 kg. After nitrous oxide inhalation, swine were intubated and ventilated with room air by the constant-volume cycled respirator (Harvard Apparatus model 607; Harvard Apparatus, Hoilliston, Mass) and anesthetized with 1.5% to 2% isoflurane. A fluid-filled cannula was placed in the left carotid artery and connected to the transducer to monitor arterial blood pressure. A great cervical vein cannula was used to infuse normal saline at a rate of 100 to 200 mL/h to replace spontaneous fluid losses and to inject drugs. Electrocardiogram and pulse oxymetry were continuously monitored.

Mechanical irritation of the pericardium may cause Bezold-Jarisch (vagal) reflex and bradycardia that can result in significant deterioration of hemodynamics; therefore, immediately before the pericardiocentesis, 1 mg of atropine was administered to suppress the vagal reflex and an additional 0.5 mg of atropine was administered when the heart rate decreased to less than 70 beats/min. After local anesthesia, an 18G epidural needle connected to a 10-mL syringe filled with contrast material was inserted from the subxyphoid toward the heart shadow under x-ray fluoroscopic guidance.¹⁸ After puncture of the pericardial membrane, the guide wire (outer

diameter = 0.81 mm) was inserted into the pericardial space, and the catheter sheath was inserted along the guide wire to the pericardial space. We used 6 types of sheaths. The size, stiffness, shape, and material of each sheath are shown in Figure 1. Sheaths were selected in accordance with the diameter of the endoscope. Six ready-made endoscopes (Olympus Medical Systems Corp, Tokyo, Japan) were used. The model number, visual angle, direction of lens, size, device ports, optical image system, and features of the endoscopes are shown in Figure 2. The endoscopes are advanced through the variety of sheaths, checking the effects of hemodynamic data, controllability, and quality of the view. We tried to maintain a clear view by regulating the amount of air and saline insufflations through the working port of the endoscope. Measured vital signs, fluoroscopic images, and endoscopic images were analyzed and evaluated after each experiment. To assess chronic effects, animals were kept alive for 2 weeks and then inspected for evidence of injuries to pericardium, lungs, and other organs.

RESULTS**Effect of Endoscope and Sheath Size on Hemodynamic Parameters**

The performance of the endoscope increases as a function of the diameter of the endoscope; however, the hemodynamics may deteriorate. Thus, the adequate diameter of the endoscope with acceptable visual images without significantly changing the hemodynamics should be determined. Representative hemodynamic data during pericardial endoscopy are shown in Figure 3. The endoscope with the largest diameter (6.9 mm in ES5) did not cause significant deterioration of hemodynamic parameters; thus, the endoscope with a diameter less than 6.9 mm is acceptable.

To obtain a clear image, design of the optomechanical device is important. Mounting a charge-coupled device (CCD) camera on the tip of the endoscope to connect directly to the objective lens significantly improved image quality (Figure 4, D, F). However, this is difficult to do with a thinner endoscope because of limitations on the miniaturization of

No	ID(F)	Model	Material	Stiffness	Shape	Check valve	Image
SH1	10	radifocus introducer-IIIH	polypropylene	soft	curved	tight	
SH2	15	hand made	polypropylene	soft	straight	tight	
SH3	21	hand made	polytetrafluoroethylene	floppy	floppy	tight	
SH4	18	capioc percutaneous catheter kit	polypropylene	hard	curved	none	
SH5	16.5	TOLOCKER Ø 5.5mm	stainless	solid	straight	loose	
SH6	33	TOLOCKER Ø 11mm	stainless	solid	straight	loose	

FIGURE 1. List of the sheaths used. Internal diameter in French, model name, material, stiffness, shape of the tip, durability of the check valve, and an image of the sheath (white scale bars = 5 cm). ID, Internal diameter; F, French.






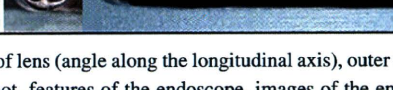
No	Model	Visual angle(°)	Direction of lens(°)	Ø OD(mm)	Device port (Ømm)	Adequate sheath	CCD on the Tip	Purpose or usage	Image	Performance
ES1	URF-P5	90	0	2.9	1.2	SH1	×	Designed for pyelo-urine tract		poor
ES2	BF-XP160F	90	0	3.25	1.2	SH1 SH2 SH5	×	Designed for tracho-bronchial tract		poor
ES3	BF-MP160F	120	0	5.0	2.0	SH2 SH5	×	Designed for tracho-bronchial tract		moderate
ES4	IPLEX FX IV8420	120	90	4.0	non	SH2 SH3 SH4	○	Designed for industrial usage, i.e., to check internal surface of pipes. Robotic controller attached		good
ES5	BF TYPE UC160F-OL8	80	35	6.9	2.0	SH3 SH4 SH6	×	Designed for tracho-bronchial tract, with ultrasonic imaging system		well
ES6	GIF-XP150N	120	0	5.5	2.0	SH3 SH4 SH5	○	Designed for trans-nasal gastro-intestine camera		good

FIGURE 2. List of the endoscopes used. Models of the endoscope, visual angle, direction of lens (angle along the longitudinal axis), outer diameter, inner diameter of utility port, adequate sheath, whether CCD camera is mounted on the tip or not, features of the endoscope, images of the endoscope (scale bars = 5 mm), and the performance of the endoscope in the pericardial space. *CCD*, Charge-coupled device; *OD*, outer diameter.

the CCD camera. Therefore, the CCD camera was mounted on the body of the thin endoscope and connected to the objective lens by a bundle of flexible optic fibers, which significantly improved image quality (Figure 4, A–C, E). Because the thickest endoscope (outer diameter = 6.9 mm) was hemodynamically tolerable, we concluded that mounting the CCD on the endoscope tip was adequate for pericardial endoscopy. Taking these results into account, we selected ES4 and ES6 as adequate for a pericardial endoscope.

The selection of the sheath was more important. To insert a large endoscope into a pericardial space, sheaths with a larger diameter are required, but ready-made larger sheaths are uncommon (SH1, SH5, SH6) and most of them are solid (SH5, SH6). Solid sheaths were unstable in positioning, and use of SH6 sometimes caused significant deterioration of hemodynamic parameters. Therefore, after insertion of the endoscope, withdrawal of the sheath was required to stabilize hemodynamic parameters (Figure 3, A). Accordingly, we prepared our handmade flexible sheath with a larger diameter (SH2, SH3, SH4), which did not cause a significant change in hemodynamic parameters (Figure 3, B). A check valve on the sheath was also important to maintain the volume of air in the pericardial space. The SH3 exhibited the best performance.

Clear Visualization

Our first achievement was to establish the method to obtain a clear view of the pericardial space by endoscopy.

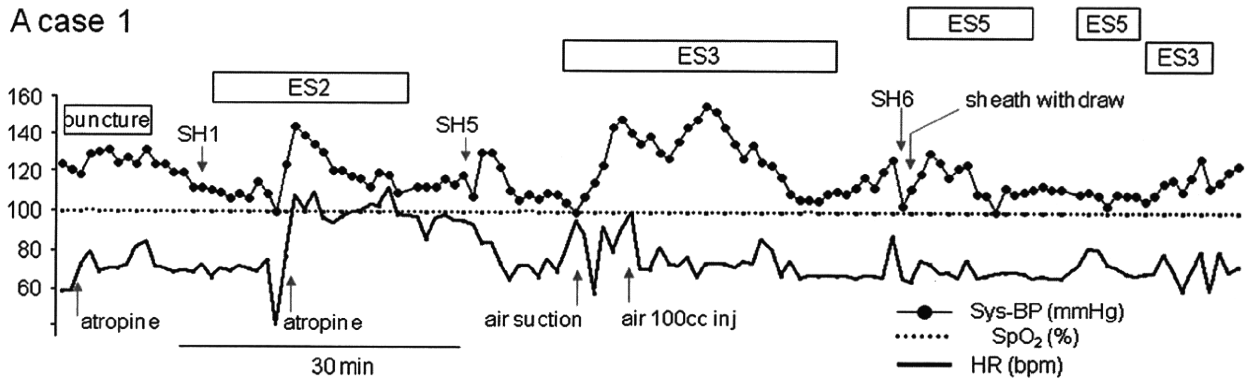
Expansion of the pericardial space by air enables us to maintain a distance from the camera to the heart surface, which is necessary for a clear view. An equal volume of saline was injected in some experiments, but a good image was not obtained and there was significant deterioration of hemodynamic parameters (Figure 3, B). Therefore, we decided to inject air to expand the pericardial space.

A larger amount of air infusion provides better vision, but on the other hand it may deteriorate hemodynamic parameters by inhibiting diastolic function of the ventricles. Injection of 100 to 200 mL of gas into the pericardial space caused no hemodynamic changes (±5 mm Hg) and allowed a stable view. In addition, resulting decreases in systolic blood pressure were less than 10 mm Hg, which is almost tolerable.

Orientation of the View

Determination of orientation of the view is important for an endoscopic-guided operation. Because of strong motion artifacts in the visual field, x-ray fluoroscopic guidance is essential to determine orientation of the tip of the endoscope. Furthermore, recognition of several landmarks of the heart can also help in understanding orientation. Infusion of 10 to 20 mL of saline and 50 to 100 mL of air into the pericardial space gives us a clear view of fluid levels. The fluid level is an important compass for horizontal

A case 1



B case 2

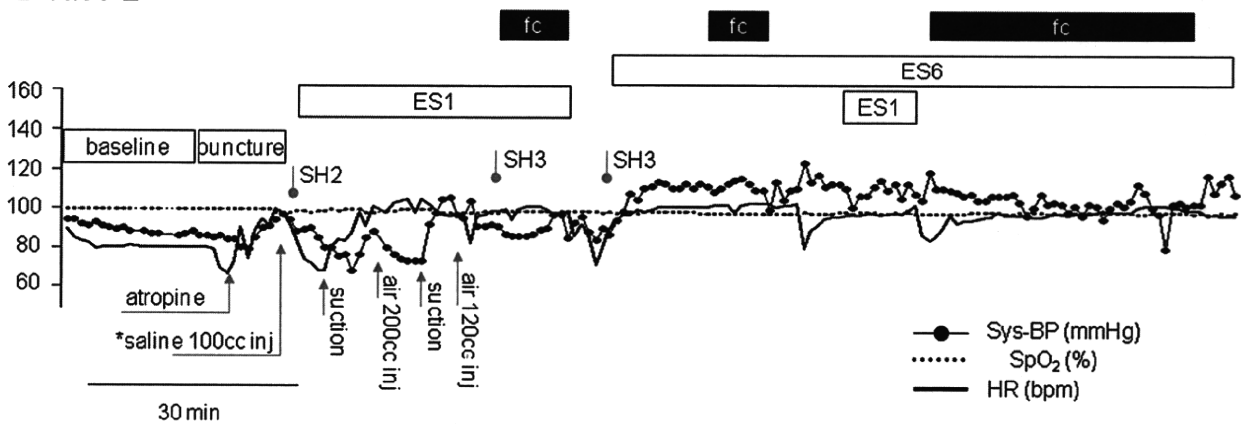


FIGURE 3. Systolic blood pressure, pulse oxymetry, and heart rate as a function of time during procedures of representative cases. Upper white bars in the graphs denote period of endoscope insertion, and black bars denote insertion of laparoscopic forceps. Upper gray arrows denote the time of insertion of each sheath, and lower gray arrows denote the timing of administration of atropine, suction, and injection of air/saline into the pericardial space. Hemodynamic parameters during procedure are well within tolerable limits. Sys-BP, Systolic blood pressure; SpO₂, pulse oxymetry; HR, heart rate; ES, endoscope; fc, forceps; SH, sheath.

direction of the visual field. Landmarks (Figure 5) in the visual field also help us to recognize the position of the tip of the endoscope. Left and right atrial appendages are clear landmarks (Figure 5, A, C, M, P, Q, S, T, U). Other heart landmarks, that is, the aortic root (Figure 5, K), pulmonary veins (Figure 5, G, N), superior vena cava (Figure 5, E), and coronary arteries (Figure 4, A–F; Figure 5, R), also give us a clue to define the orientation. Adjacent organs—the lung, diaphragmatic membrane (Figure 5, I, W), and puncture site (Figure 5, V)—can be good landmarks.

Control of Endoscopes

It is an advantage to understand the movement of the endoscope to stabilize the tip of the device at the exact location. After the modified Seldinger technique, the anteroapical portion of the pericardium was penetrated by sheaths. By advancing and retracting the endoscope, the tip of the endoscope simply moved forward and backward along the anterior interventricular groove. In this manner, the endoscope was straight, the x-ray showed an “I-shape”

configuration, and the heart was observed as in an upward-viewing manner (apex to base direction, Figure 6, F). As the endoscope was advanced, the left anterior descending coronary artery (Figure 4, A, E, F), left atrial appendage (Figure 4, E; Figure 5, A, M, S, T), and aortic root were observed (Figure 5, K). By bending the endoscopic tip toward the right side, the outflow tract and right ventricle (Figure 5, O) were observed; by bending toward the left, the left pulmonary veins could be observed (Figure 5, G). However, this view was unstable; because the support (backup) of the shaft was only a shallow interventricular groove, the tip was easily dislodged. Therefore, another endoscopic control is required to observe the whole heart.

When we gently advanced the endoscope in the I-shape configuration under a fluoroscopic guide (Figure 6, A, F), the tip was trapped at the position along the roof (cranial end, Figure 6, B) of the pericardial space, between the right ventricular outflow tract and the left atrial appendage. At this position, if we rotated the shaft clockwise and advanced the endoscope with maximally bending the tip

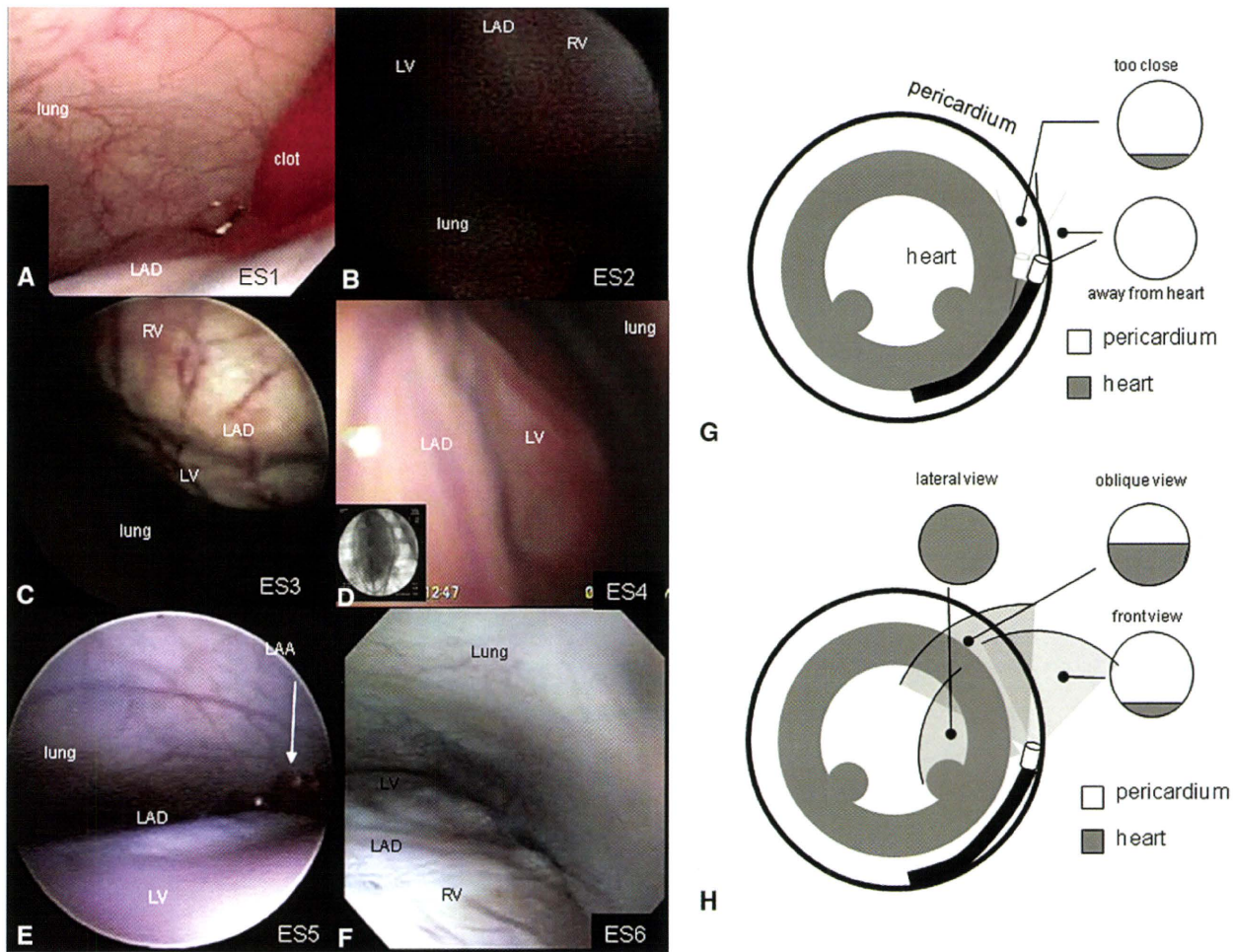


FIGURE 4. A–F, Representative images of left anterior descending artery observed by each endoscope (denoted right bottom, number corresponding to it in Figure 1). It is difficult to front-view the endoscope with a narrow visual angle (A, B). Images of the endoscope without mounting the CCD on the tip (C, E) are fuzzy. Images of the endoscope with the CCD on the tip (D, F) are vivid. G, H, Schematic diagram of spatial configuration of endoscope in the pericardial space and its visual field. G, If the head of the front-view endoscope is directed to the heart surface, the objective lens gets too close to the heart surface. On the other hand, if the endoscope is tipped away from the heart surface, the visual field of the endoscope also tips away from the heart. H, The relation between the visual field and the direction of the objective lens. LAD, Left anterior descending artery; LV, left ventricle; ES, endoscope; RV, right ventricle.

(Figure 6, C), the tip of the endoscope could be advanced into the right side of the pericardial space. The middle shaft was turned around at the caudal roof of the pericardium, resulting in a so-called inverted U-shape right-side configuration (Figure 6, D, E, G, H), allowing the heart to be observed as in a downward-viewing manner (base to apex direction). On the other hand, if we rotated the shaft counterclockwise and advanced the endoscope, the tip of the endoscope could go through the left side of the heart, and a so-called inverted U-shape left-side configuration could be achieved. By use of the inverted U-shape configurations, we could observe every portion of the epicardium (Figure 6, H; Video 1).

To effectively control pericardial endoscopy, it is important to take into account the position of backup of the shaft and fulcrum at the point of bending. First, the shaft was

fixed at the puncture point of the pericardium. In the I-shape configuration, the shaft was moderately backed up by the anterior interventricular groove, the rotation of the shaft did not help steering devices, and the fulcrum point of bending was only the epicardium. Therefore, it was difficult to keep a distance between the objective lens and the epicardial surface (Figure 4, G), resulting in loss of focus and significant halation (Figure 5, X). However, when the tip was advanced and bent, the visual field was directed toward the pericardium and kept a distance from the epicardial surface (Figure 4, G). Finally, in the inverted U-shape configuration, the middle of the shaft was strongly backed up by the whole pericardium and we could steer the devices by rotating the shaft. This configuration enabled us to keep an appropriate distance from the epicardial surface (Figure 4, H; Video 2).

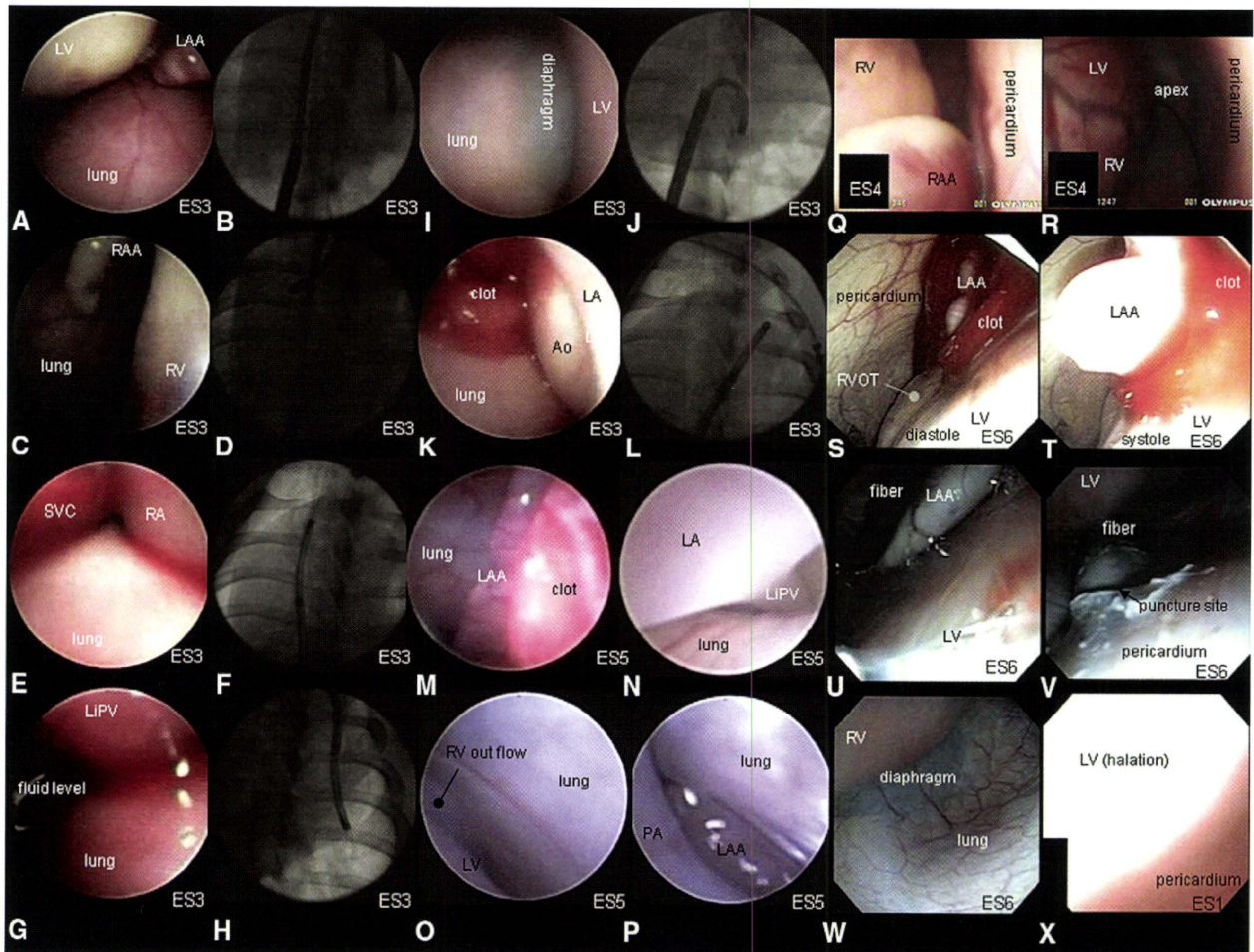


FIGURE 5. Representative images obtained by endoscopy and fluoroscopy. Endoscopic images (A, C, E, G, I, K) obtained by ES3 and corresponding fluoroscopic images (B, D, F, H, J, L, respectively). A, Left atrial appendage and lateral wall of left ventricle. C, Right atrial appendage and lateral wall of right ventricle. E, Superior vena cava and right atrium. G, Left inferior pulmonary vein. I, Pericardium at the diaphragm looks pale compared with pericardium at the lungs. K, Left ventricular outflow tracts. Aortic root and left atrium can be observed. M–P, Endoscopic images obtained by ES5. Left atrial appendage (M, P), left inferior pulmonary vein (N), and pulmonary artery outflow tract (O, P). Q, R, Endoscopic images obtained by ES4. Right atrial appendage (Q), right ventricle (Q, R), and ventricular apex (*apex*, R). S–W, Endoscopic images obtained by ES6. S, T, Sequential image showing dynamic motion of left atrial appendage. U, Left atrial appendage and body of fiber itself. V, Pericardial puncture site and the body of fiber itself. W, Pericardium at the diaphragm. The quality of the images obtained by ES6 is superior to that obtained by ES3. X, Image obtained by ES1. By using the front-view ES with a narrow visual angle, it is difficult to observe the heart surface without significant halation. Ao, Aortic; ES, endoscopy; LA, left atrium; LAA, left atrial appendage; LIPV, left inferior pulmonary vein; LV, left ventricle; PA, pulmonary artery; RA, right atrium; RAA, right atrial appendage; RV, right ventricle; S, diastole; SVC, superior vena cava; T, systole.

Feasibility of Minor Surgery

We tested the feasibility of endoscope-guided small operations in the pericardial space. To simulate transplantation of stem cells into the myocardium from the epicardium, we injected Indian ink into the epicardium via endoscope. A 1-mL syringe with 0.2 mL of Indian ink was connected to a 22G needle for endoscopy (NA-201SX-4022; Olympus, Tokyo, Japan). The needle tip was insulated by external Teflon tubing to avoid injury to the coronary vessels. The needle was attached to the surface of the left ventricular free wall via a utility port (Figure 7, A). After positioning of

the tip, the internal needle was protruded into the myocardium, and then Indian ink was injected without severe hemorrhage (Figure 7, B). By protruding the external tube, the objective lens and surface of the heart were stabilized to significantly reduce strong motion artifacts, and adequate working distance was achieved (Figure 7, C).

Rigid laparoscopic forceps are essential for endoscope-guided surgery; however, such rigid forceps may compress the heart and deteriorate hemodynamic parameters. Therefore, a flexible endoscope (ES6) and rigid laparoscopic forceps (Figure 7, E) were inserted simultaneously to perform

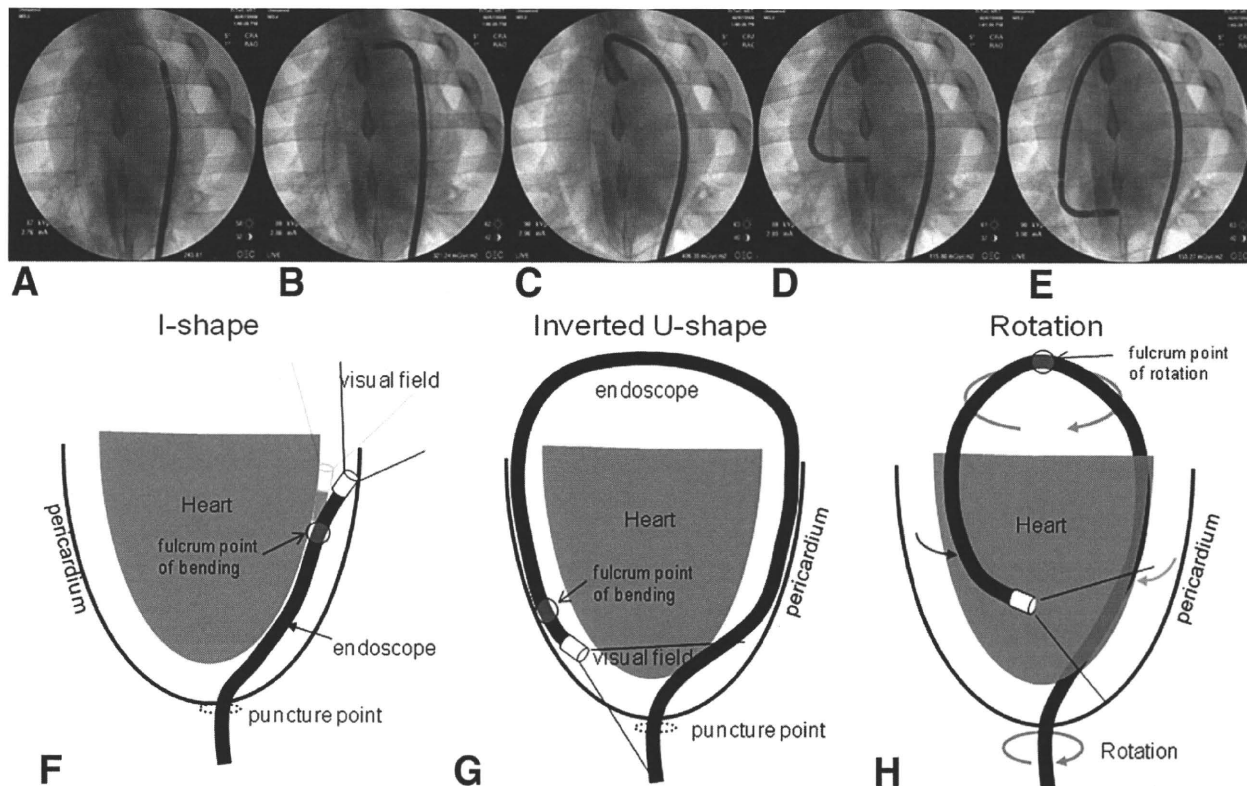


FIGURE 6. A–E, Sequential fluoroscopic images during changing I-shape configuration to inverted U-shape configuration. See details in text. F–H, Schematic diagram of I-shape configuration, inverted U-shape configuration of pericardial endoscope, and how to steer the tip of the endoscope in the pericardial space.

minor surgery (Figure 7, F–H). A needle-type pacing electrode (Figure 7, I) was transplanted into the left ventricular free wall by use of ES6 (Figure 7, F–H). Transplantation was successfully performed without significant hemodynamic change (Figure 7, J–L; Video 2).

Complications

Because pericardial endoscopy is the leading minimally invasive technique, the safety of this procedure is our main concern. In the process of puncture by the Seldinger technique, there were no complications, such as hemorrhages, pneumothorax, perforation of left ventricle, or other injuries. During the whole procedure, we could handle the devices in and out numerous times with no changes in blood pressure, pulse oxymetry data, or heart rate (Figure 3) for more than 1 hour. The injection of more than 200 mL of air into the pericardial space suppresses blood pressure by 5 to 10 mm Hg, but blood pressure recovers immediately by removing air from the space via endoscopic utility port.

In terms of chronic phases, pericardial inflammation was evaluated 2 weeks after the operations. There were no macroscopic injuries, coronary stenosis by coronary angiogram, hemorrhages, or adhesion of pericardium (Figure 7, D).

DISCUSSION

Selection of Best Endoscope

Because the first priority for pericardial endoscopy is a clear image, an endoscope with a CCD camera on the tip is essential. In popular endoscopes, the objective lens is usually positioned toward an anterior direction (forward-view, ES1, ES2, ES3, ES6). When the endoscope is inserted into the pericardial space, a shaft of the endoscope usually fits along the curve of the epicardial surface, but the objective lens faces toward a tangent direction to the epicardial surface and away from the surface of the heart (Figure 4, G). It is reasonable to imagine that positioning the objective lens in a 30- to 60-degree interior oblique direction may be another option (Figure 4, H). From an optomechanical point of view, it is difficult to position the lens and CCD complex on the thin tip of endoscopes, although a lens with a 90-degree direction (lateral-view, ES4) can be achieved. Also, so-called fish-eye lenses or wider visual angle lenses (ES3, ES4, ES6) enable observation of the heart surface, even if the distance between the heart and the device is not sufficient.

A diameter less than 6.9 mm with a soft shaft is acceptable, and utility port is necessary for controlling air and devices. Among the ready-made endoscopes, the ES6 showed

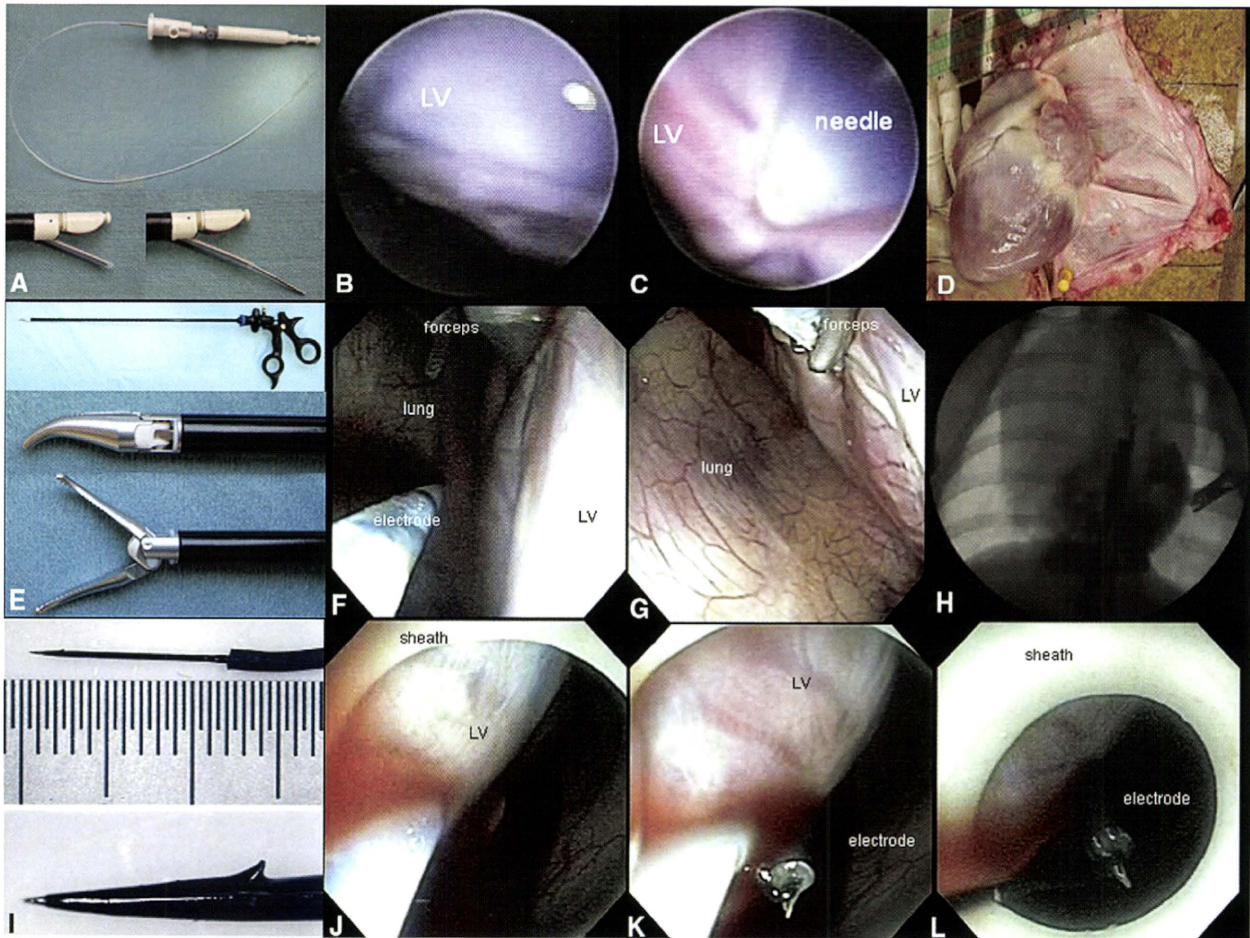


FIGURE 7. A–C, Indian ink was injected into the left ventricular epicardium with a needle. B, Immediately after injection of Indian ink, there was no active bleeding. D, Two weeks after the pericardial endoscopy, there was no coronary injury and no marked adhesion of pericardium. E, Laparoscopic forceps used. F, G, Endoscopic (ES6) images during implantation of pacing lead (I) in the left ventricular muscle by using laparoscopic forceps and fluoroscopic images during procedure (H). Implanted pacemaker lead immediately after the implantation (J–L). LV, Left ventricle.

the best performance. The ES4 also showed good performance, but there is no utility port for intervention.

Selection of Best Sheath

A certain length of the sheath should be positioned in the pericardial space to obtain back-up support for intervention. By advancing the sheaths, the direction of the sheath is usually perpendicular to the heart surface. A solid sheath causes significant compression of the heart surface and deterioration of hemodynamic parameters. Thus, a floppy sheath is suitable for pericardial endoscopy. Furthermore, to maintain the amount of air within the pericardial space, a check valve at the top of the sheath is essential. Taking this into account, we selected SH4 as the best sheath for pericardial endoscopy.

Stabilization of Motion Artifacts

Stabilization of strong motion artifacts is important. Keeping a distance from the heart surface by use of the in-

verted U-shape configuration can help stabilize the visual field. Gentle compression of the heart by a rigid manipulator, such as sheaths and laparoscopic forceps, can also stabilize the heartbeat.

Optimization of the Tools

Although we demonstrated the feasibility of the pericardial endoscope by ready-made endoscopes, optimization of the tools should be required. The ES6 is almost acceptable as a pericardial endoscope if we have well-designed forceps for interventions through the utility port. On the other hand, further optimization of the manipulator should be done for pericardial interventions, such as an optimized tool for a cell-delivery system, epicardial pacemaker implantation, and curving of the tip to fit along the heart curvature. The design for the sheath should also be optimized. The optimal material, stiffness, and curve of the sheath remain to be elucidated.

Limitations

Before application for human use, the pericardial endoscopic system should be optimized, and further experiments should be done in other conditions. For example, we did not try the system on an animal with heart failure; therefore, the feasibility of the procedure in the patient with severe heart failure is still undetermined.

We performed the experiment under general anesthesia with respirator support, but for humans this procedure could be performed with local anesthesia. However, in patients with congenital pericardial defect, of which there is a prevalence of 0.0001%¹⁹ to 0.044%,²⁰ infusion of the gas may cause pneumothorax, so respirator support should be required in such cases.

During this procedure, coincidental occurrence of ventricular fibrillation should be carefully monitored. If this occurs, immediate suction of the gas should be required to perform successful external defibrillation.

It was difficult to observe the posterior surface of the heart because of the limited space between the posterior wall of left atrium and the spine. If the target is the posterior portion of the heart, a lateral position of the patient may gain space and avoid puddling at the focus area. Further experiments should be done for safer procedures.

Clinical Applications

The future of this new technique relies on optimizing its use in humans. Previous studies have demonstrated the effective use of the pericardial approach in the human body, and the device itself is already well known and used clinically. Therefore, there are no obstacles to human application. This method enables us to reach epicardial areas and deep into the myocardium to focus on ablation and implantable cardioverter/defibrillator lead placement in a minimally invasive way. In the present study, we infused air into the pericardial space. However, there is less chance of causing air embolism and significant mediastinal emphysema with carbon dioxide compared with air. For clinical application, infusion of carbon dioxide gas is considered to be safer in this system.

Moreover, in cardiac stem cell therapy, there is no standard method of stem cell transplantation. Transplantation via coronary vessels may not deliver the cells to the appropriate location in the heart tissue, may occlude coronary vessels, and may generate additional myocardial infarctions.⁷ Direct injection into the myocardium from an endocardial site via a needle devised on the tip of a catheter using an electroanatomic mapping system (NOGA System, Biosense Webster, Markham, ON, Canada)⁶ is similar to the common catheter ablation procedure. Although the catheter procedure is safe and can be performed repeatedly, the injected cells may backflush into the left ventricular cavity via needle trajectory and disseminate into the

systemic circulation, causing systemic microembolizations. From this point of view, injection of the cells from the epicardial surface is secure. However, open chest surgery is required to avoid coronary vessels. Pericardial endoscopy-guided cellular transplantation from the epicardial surface can be a major method for stem cell transplantation.

CONCLUSIONS

Our experiment has established a new and simple method for obtaining a clear view of the pericardial space with the use of pericardial endoscopy. The percutaneous subxyphoid approach using the Seldinger technique was useful and safe. An x-ray fluoroscopic guide was necessary to steer the endoscope in the pericardial space. We have shown short- and long-term safety with regard to hemodynamic changes, infections, and adhesion of pericardium. Pericardial endoscopy can introduce a new era of technology for cardiac surgeons and cardiac interventionists.

The authors thank Olympus Corporation for technical advice and Satoshi Ogawa MD, PhD, and Toshiaki Satoh, MD, PhD, for medical advice.

References

1. Gruntzig AR, Senning A, Siegenthaler WE. Nonoperative dilatation of coronary artery stenosis: percutaneous transluminal coronary angioplasty. *N Engl J Med.* 1979;301:61-8.
2. Gallagher JJ, Svenson RH, Kasell JH, German LD, Bardy GH, Broughton A, et al. Catheter technique for closed-chest ablation of the atrioventricular conduction system. *N Engl J Med.* 1982;306:194-200.
3. Scheinman MM, Morady F, Hess DS, Gonzalez R. Catheter-induced ablation of the atrioventricular junction to control refractory supraventricular arrhythmias. *JAMA.* 1982;248:851-5.
4. Abraham WT, Fisher WG, Smith AL, Delurgio DB, Leon AR, Loh E, et al. Cardiac resynchronization in chronic heart failure. *N Engl J Med.* 2002;346:1845-53.
5. Cribier A, Eltchaninoff H, Bash A, Borenstein N, Tron C, Bauer F, et al. Percutaneous transcatheter implantation of an aortic valve prosthesis for calcific aortic stenosis: first human case description. *Circulation.* 2002;106:3006-8.
6. Perin EC, Dohmann HF, Borojevic R, Silva SA, Sousa AL, Mesquita CT, et al. Transendocardial, autologous bone marrow cell transplantation for severe, chronic ischemic heart failure. *Circulation.* 2003;107:2294-302.
7. Vulliamt PR, Greeley M, Halloran SM, MacDonald KA, Kittleson MD. Intra-coronary arterial injection of mesenchymal stromal cells and microinfarction in dogs. *Lancet.* 2004;363:783-4.
8. Breitbach M, Bostani T, Roell W, Xia Y, Dewald O, Nygren JM, et al. Potential risks of bone marrow cell transplantation into infarcted hearts. *Blood.* 2007;110:1362-9.
9. Kikuchi K, McDonald AD, Sasano T, Donahue JK. Targeted modification of atrial electrophysiology by homogeneous transmural atrial gene transfer. *Circulation.* 2005;111:264-70.
10. Ota T, Degani A, Zubiate B, Wolf A, Choset H, Schwartzman D, et al. Epicardial atrial ablation using a novel articulated robotic medical probe via a percutaneous subxyphoid approach. *Innovations Phila Pa.* 2006;1:335-40.
11. Soejima K, Couper G, Cooper JM, Sapp JL, Epstein LM, Stevenson WG. Subxyphoid surgical approach for epicardial catheter-based mapping and ablation in patients with prior cardiac surgery or difficult pericardial access. *Circulation.* 2004;110:1197-201.

12. Soejima K, Stevenson WG, Sapp JL, Selwyn AP, Couper G, Epstein LM. Endocardial and epicardial radiofrequency ablation of ventricular tachycardia associated with dilated cardiomyopathy: the importance of low-voltage scars. *J Am Coll Cardiol.* 2004;43:1834-42.
13. Maisch B, Bethge C, Drude L, Hufnagel G, Herzum M, Schonian U. Pericardioscopy and epicardial biopsy—new diagnostic tools in pericardial and perimyocardial disease. *Eur Heart J.* 1994;15(Suppl C):68-73.
14. Seferovic PM, Ristic AD, Maksimovic R, Tatic V, Ostojic M, Kanjuh V. Diagnostic value of pericardial biopsy: improvement with extensive sampling enabled by pericardioscopy. *Circulation.* 2003;107:978-83.
15. Nazarian S, Kantsevov SV, Zviman MM, Matsen FA 3rd, Calkins H, Berger RD, et al. Feasibility of endoscopic guidance for nonsurgical transthoracic atrial and ventricular epicardial ablation. *Heart Rhythm.* 2008;5:1115-9.
16. Gerosa G, Bianco R, Buja G, di Marco F. Totally endoscopic robotic-guided pulmonary veins ablation: an alternative method for the treatment of atrial fibrillation. *Eur J Cardiothorac Surg.* 2004;26:450-2.
17. Zenati MA, Bonanomi G, Chin AK, Schwartzman D. Left heart pacing lead implantation using subxiphoid videopericardioscopy. *J Cardiovasc Electrophysiol.* 2003;14:949-53.
18. Spodick DH. The technique of pericardiocentesis. When to perform it and how to minimize complications. *J Crit Illn.* 1995;10:807-12.
19. Southworth H, Stevenson CS. Congenital defects of the pericardium. *Arch Intern Med.* 1938;223-40.
20. Van Son JA, Danielson GK, Schaff HV, Mullany CJ, Julsrud PR, Breen JF. Congenital partial and complete absence of the pericardium. *Mayo Clin Proc.* 1993; 68:743-7.

000 Safety and efficacy of pericardial endoscopy by percutaneous subxyphoid approach in swine heart in vivo

Takehiro Kimura, MD, Shunichiro Miyoshi, MD, PhD, Seiji Takatsuki, MD, PhD, Kojiro Tanimoto, MD, PhD, Kotaro Fukumoto, MD, PhD, Kyoko Soejima, MD, PhD, and Keiichi Fukuda, MD, PhD, Tokyo and Kawasaki, Japan

As the pioneer of the novel minimally invasive surgery, we have demonstrated the safety and feasibility of pericardial endoscopy. We have established the techniques to obtain clear images by selecting appropriate devices in swine and succeeded in performing interventions such as cell transplantation and pacemaker lead implantation with no complications.